IET Control Theory & Applications

Research Article

IET Journals
The Institution of Engineering and Technology

Stabilisation of event-triggered-based neural network control system and its application to wind power generation systems

ISSN 1751-8644
Received on 6th March 2019
Revised 4th October 2019
Accepted on 20th January 2020
E-First on 12th May 2020
doi: 10.1049/iet-cta.2019.0246
www.ietdl.org

Lakshmanan Shanmugam[1], Prakash Mani[1], Young Hoon Joo[1] ✉

[1]*Research Center for Wind Energy Systems, Kunsan National University, Gunsan, Chonbuk 573-701, Republic of Korea*

✉ *E-mail: yhjoo@kunsan.ac.kr*

Abstract: This study addresses the event-triggered (ET)-based stabilisation problem of neural-network-based control system (NNBCS) and illustrates the direct application to wind power generation system. In this regard, the novel ET-based controller algorithm is designed for NNBCS instead of sampled data controller (sampling will be initiated at a fixed rate regardless whether it is required or not) which reduces the computation complexity by avoiding the unnecessary details over the transmission. The novel stability and stabilisation conditions are expressed in terms of linear matrix inequalities that are derived through constructing the time-dependent Lyapunov functional candidate. For deepening the knowledge in the outcomes of the proposed conditions, the study numerically evaluates the dynamic models such as variable-speed wind turbine drive system, permanent magnet synchronous motors model and traditional inverted pendulum model and validates the effectiveness of the proposed controller scheme. Finally, a comparison result shows the superiority of the derived conditions.

Nomenclature

B_s	shaft damping
J_T and J_g	turbine and generator inertia
K_s	shaft compliance
Q	shaft torque
Q_A	input wind torque
Q_E	generator torque
$\mathscr{R}$	blade length
V	wind velocity,
ω_t	turbine angular velocity
ω_g	generator angular velocity
ρ	air density

1 Introduction

The world without modern technologies is likely to be the home without doors, in this situation, the requirement of energy is rapidly increasing. Lots of technological developmenets are made for the production, renewable and minimise the consumption via green energies which include wind farm, solar energy, hydro, bio-masss and they proved the importance of saving the natural resources. However, it is not possible to implement every minute details into real-world systems because of economic crisis [1–3]. In this regard, the fundamental research on these renewable energies is always of great interest because of cost-effective and time complexity when compared to practical implementation. For instance, in a wind power generation system (WPGS), the investigation of the controllers have a significant role for pitch and yaw components. Mathematical modelling of real-world problems via differential equations will help to reveal the system properties and proven the significance of parameters. Among various green energies, we aim to investigate the WPGS which is one of the main sources of electricity. In the literature, WPGSs are modelled into the set of non-linear differential equations that acquires the information about the productivity of energy. In addition, numerous controllers have been proposed and proved the stable performance of the wind turbines (see for example [4–8]). In general, improvements are still necessary in order to configure the stable performance and optimise the leakages. Hence, in this work, we theoretically design the event-triggered (ET)-based control scheme for the generalised non-linear differential model and validate them with WPGSs.

Computational intelligence models that include artificial neural networks (ANNs) are used to train and model the non-linear and complex patterns, which helps to predict the complete information on real-world problems [9, 10]. In contrast to the existing approximations, any smooth continuous function that lies in the compact domain can be approximated to an arbitrary accuracy via ANNs. For example, in [11], authors have investigated the stability and the optimised performance for the sampled-data neural-network-based control system (NNBCS). In general, NNBCS comprises the non-linear plant and neural-network-based controller in the closed-loop form and they adapted the three-layer fully connected feedforward neural network (TLFCFFNN) as an approximation tool. In that work, two major approaches have been combined, i.e. linear matrix inequality (LMI) and genetic algorithm to obtain the largest sampling period and connection weights of the neural network. Similar to the above work, authors in [12–14] have proposed the delay-dependent stabilisation conditions based on novel piecewise Lyapunov function. Particularly in [13], authors have proposed the exponential stabilisation conditions for NNBCS based on time-dependent Lyapunov functional (TDLF) which has proven the asymptotical stability of the closed-loop system.

The common feature shared by these works is sampled-data TLFCFFNN controller (time-triggered control, the control task is performed in a periodic way, for more details, refer [15, 16]). However, in some situations, control task will be operated in all cases, i.e. sampling will be initiated at a fixed rate regardless whether it is required or not which results in the wastage on both computation and energy resources. To overcome this restriction, the ET controller is the best option which automatically makes a decision regarding the execution of the control task based on predefined ET condition rather than some fixed time. Once the ET condition is disturbed at some instant, which implies that the event is triggered, the control task will be immediately initiated. A detailed analysis of time-triggered and ET controllers are reported in [17–27]. Also, with reference to the works in [11–13], all the authors have designed the sampled-data neural-network-based control (SDNNC) for only non-linear physical experiment problem on the cart and inverted pendulum and to the different aspect, the main motivation of our work relies on the investigation of non-linear WPGS via the proposed ET NNBCS (ETNNBCSs).

Motivated by the aforementioned discussion, theoretical investigation of ETNNBCSs needs much attention, so far only one research report has been published in the literature when compared

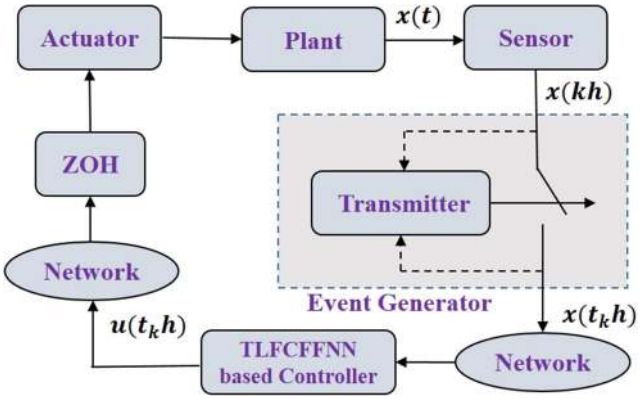

Fig. 1 *The schemetic diagram of ET-TLFCFFNN scheme*

to SDNNC. In particular, the authors in [28] have introduced ET scheme for TLFCFFNN-based controller and established the stabilization criteria based on Lyapunov functional. However, in this paper, the problem of stabilisation for ETNNBCS is investigated. In addition, an ET scheme is introduced into the neural-network-based controller which include the transmission delay $\tau(t)$ with both lower and upper bounds but the authors in [28] have considered only the upper bound which needs to be improved. The proposed controller scheme guarantees the globally asymptotically stable for the given closed-loop system. For complete information, the motivation of the present work is that the non-linear plants say, variable-speed wind turbine drive system and permanent magnet synchronous motor (PMSM) ([29, 30]) are adapted for the investigation and the suitable ET-based neural network control is designed. The sufficient condition in terms of strict LMIs for considered ETNNBCS is derived through suitable time-dependent LKF which include the information of lower and upper bound of the transmission. Finally, the proposed sufficient conditions are validated through numerical examples.

Notation: We start with an introduction of some common notations used in the main results. Let $\mathbb{R}^n$ be Euclidean n-dimensional space and $\mathbb{R}^{n\times m}$ represents $n\times m$ real matrix. $*$ denotes symmetric term in the symmetric matrix. $X > 0 (\geq 0) \in \mathbb{R}^{n\times n}$ denotes positive matrix (positive semi-definite matrix) with $n\times n$ and I denotes the identity matrix with appropriate dimension.

2 Preliminaries and problem formulation

Now, consider the non-linear plant (model) with control form as follows:

$$\dot{x}(t) = f(x(t), u(t)), \tag{1}$$

here, $x(t) \in \mathbb{R}^n$ denotes the state vector of the non-linear model (1) and the control input $u(t) \in \mathbb{R}^m$. The vector form of non-linear function is $f(\cdot): \mathbb{R}^n \times \mathbb{R}^m \longrightarrow \mathbb{R}^n$. The following is the similar model proposed in [11–13],

$$\dot{x}(t) = \sum_{i=1}^{p} \omega_i(x(t))(A_i x(t) + B_i u(t)), \tag{2}$$

with $A_i \in \mathbb{R}^{n\times n}$ and $B_i \in \mathbb{R}^{n\times m}$ are known real matrices. p denotes the positive integer, and $\omega_i(x(t))$ must satisfy the following condition:

$$\sum_{i=1}^{p} \omega_i(x(t)) = 1,\ \omega_i(x(t)) \in [0\ 1],\ i = 1, \ldots, p\,. \tag{3}$$

Remark 1: The authors in [11] have introduced a sampled-data TLFCFFNN-based controller say, SDNNC to continuous time non-linear plant and derived the stability conditions based on Lyapunov stability which guarantees asymptotically stability. As an improvement, in [12, 13], authors have been derived improved stabilisation conditions based on input delay approach and TDLF approach. Compared with the existing results, we inspired to design the ET-TLFCFFNN controller as in $u(t)$ that can be able to acquire the information more accurately than sampled-data TLFCFFNN.

The ET communication-based TLFCFFNN scheme of the plant is consistitng of sensor, event generator, TLFCFFNN-based controller and actuator, which is shown in Fig. 1. Inspired by the recent works on ET scheme in [22] with their preliminary assumptions in this work, the current transmitted state is denoted by $x(t_k h) = [x_1(t_k h), x_2(t_k h), \ldots, x_n(t_k h)]^{\mathrm{T}}$ at time instant $t_k h$. Here, the next triggered instant is calculated as given below

$$\begin{aligned} t_{k+1}h = t_k h + \min_m \big\{ mh \mid e^{\mathrm{T}}(i_k h)\Phi e(i_k h) \\ \geq \epsilon x^{\mathrm{T}}(t_k h)\Phi x(t_k h) \big\}\,. \end{aligned} \tag{4}$$

Here, h is sampling period, $e(i_k h)$ denotes error between the state $x(i_k h)$ at current sampling instant and the state $(x(t_k h))$ at the latest transmitted sampling instant, i.e. $e(i_k h) = x(i_k h) - x(t_k h)$, $i_k h = t_k h + mh$, $m \in \mathbb{N}$ and $0 \leq \epsilon < 1$ is scalar and $\Phi > 0$ is weight matrix.

The ET-TLFCFFNN controller for (2) is designed as follows

$$u(t) = \sum_{j=1}^{n_{\mathrm{h}}} \hat{m}_j(x(t_k h))K_j x(t_k h), \quad t \in \Xi \triangleq \left[t_k h + \tau_{t_k}, t_{k+1}h + \tau_{t_{k+1}}\right), \tag{5}$$

where

$$K_j = \begin{bmatrix} k_{1,j} & k_{2,j} & \cdots & k_{n,j} \\ k_{n+1,j} & k_{n+2,j} & \cdots & k_{2n,j} \\ \vdots & \vdots & \cdots & \ddots \\ k_{(m-1)n+1,j} & k_{(m-1)n+2,j} & \cdots & k_{mn,j} \end{bmatrix},$$

$$\hat{m}_j(x(t_k h)) = \frac{t_{\mathrm{f}}\left(\sum_{i=1}^{n} \hat{m}_{j,i} x_i(t_k h) - b_j\right)}{\sum_{a=1}^{n_{\mathrm{h}}} t_{\mathrm{f}}\left(\sum_{c=1}^{n} \hat{m}_{a,c} x_c(t_k h) - b_a\right)} \in [0\ 1],$$

$$t_{\mathrm{f}}\Big(\sum_{i=1}^{n} \hat{m}_{j,i} x_i(t_k h) - b_j\Big) \geq 0,\ j = 1, 2, \ldots, n_{\mathrm{h}}\,.$$

Here, $\hat{m}_{j,i}$ represents the connection weight between the jth hidden node and ith input node. $k_{a,j}$ denotes the connection weight between the ath output node and the jth hidden node. b_j denotes the bias for the jth hidden node. $t_f(.)$ denotes the activation function. n_h denotes the number of hidden nodes. τ_{t_k} denotes the transmission delay.

For the computational convenience, we divide the whole interval Ξ into sampling sub-intervals $\Xi_m = [i_k h + \tau_{i_k}, i_k h + h + \tau_{i_k+1})$ i.e.

$$\Xi = \cup\, \Xi_m \tag{6}$$

where $i_k h = t_k h + mh$, $m = 0, 1, \ldots, t_{k+1} - t_k - 1$ means the sampling instants from the current transmitted sampling instant $t_k h$ to the future transmitted sampling instant $t_{k+1}h$; if m takes the values of $t_{k+1} - t_k - 1$ then $\tau_{i_{k+1}} = \tau_{t_{k+1}}$, otherwise $\tau_{i_k} = \tau_{t_k}$. The illustration of sub-intervals as in the Fig. 2. Now, we define a function

$$\tau(t) = t - i_k h,\ t \in \Xi_m \tag{7}$$

where $\tau(t)$ denotes the induced delay that includes the network transmission delays which satisfies the following condition

$$0 \leq \tau_L = \inf_m \{\tau_{i_k}\} \leq \tau(t) \leq h + \sup_m \{\tau_{i_k+1}\} = \tau_U\,. \tag{8}$$

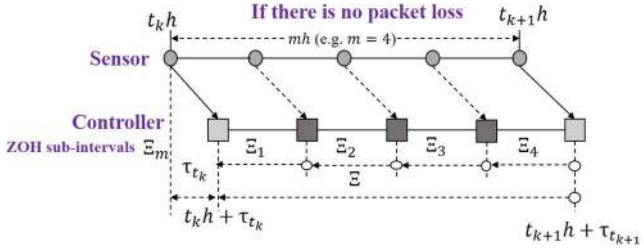

Fig. 2 *Illsuration of subintervals Ξ_m with ZOH holding [22]*

From (7), we now re-design the controller as follows,

$$u(t) = \sum_{j=1}^{n_h} \hat{m}_j(x(t_k h))K_j[x(t-\tau(t)) - e(i_k h)],\ t \in \Xi_m\,. \tag{9}$$

From (2) and (9), we can express as a closed-loop system in the following form

$$\begin{aligned}\dot{x}(t) = \sum_{i=1}^{p}\sum_{j=1}^{n_h} \omega_i(x(t))\hat{m}_j(x(t_k h))\big(A_i x(t) \\ + B_i K_j[x(t-\tau(t)) - e(i_k h)]\big)\end{aligned} \tag{10}$$

To evaluate the system performance, we have consider the following cost function as defined in [11]

$$J = \int_{t_0}^{\infty} \begin{bmatrix} x(s) \\ u(s) \end{bmatrix}^{\mathrm{T}} \begin{bmatrix} J_1 & J_2 \\ * & J_3 \end{bmatrix} \begin{bmatrix} x(s) \\ u(s) \end{bmatrix} \mathrm{d}s \tag{11}$$

where J_1, J_2 and J_3 are the given matrices with

$$\begin{bmatrix} J_1 & J_2 \\ * & J_3 \end{bmatrix} > 0.$$

We will utilise the following Lemma [31], for deriving the main results for the proposed model (10).

Lemma 1 (Matrix Cauchy inequality): For any $x, y \in \mathbb{R}^n$ and there exist a matrix $R > 0$ such that the following inequality holds

$$2x^{\mathrm{T}}y \le x^{\mathrm{T}}R^{-1}x + y^{\mathrm{T}}Ry\,.$$

Based on the non-linear model (2), ET-based control scheme (9) and the cost function (11), this brief is dedicated to the following ET-TLFCFFNN problem.

Problem 1: Given the non-linear system (1), to asymptotically stabilise the states of the closed loop system with the following design objectives.

• The designed ET-TLFCFFNN scheme ensure that the states $x(t)$ is closely convergent to the origin under the gain matrices $K_j\,(j = 1, \ldots, n_h)$.

• Under the cost function (11) and derived sufficient conditions, the minimised value of the cost function is determined under given initial conditions $x(t_0)$.

3 Main results

This section comprises the derivation of stability and stabilisation criteria in terms of theorems based on suitable TDLF under the ET-TLFCFFNN controller (9) that provides a solution to Problem 1.

3.1 Stability analysis

Theorem 1: For any given positive scalars τ_L, τ_U, and constants α_c, β_c, γ_c, $\lambda_c\,(c = 1, 2)$, and ϵ. If there exist the positive symmetric matrices P, R_1, R_2, S, $X_5\,Q \in \mathbb{R}^{n\times n}$, symmetric matrix G, any matrices X_1, X_2, X_3, X_4, M_r and $N_r, (r = 1\ldots4)$ which satisfy the following inequalities $(i = 1, \ldots, p$ and $j = 1, \ldots, n_h)$ then the system (10) is said to be asymptotically stable

$$\Psi^{ij\tau_L} < 0, \tag{12}$$

$$\Psi^{ij\tau_U} < 0. \tag{13}$$

(see equation below)
(see equation below)

All entries of $\Psi^{ij\tau_L}$ and $\Psi^{ij\tau_U}$ are given in Appendix 1.

In addition, if the proposed model (10) is asymptotically stable then their corresponding value of the cost function (11) must satisfy the following inequality

$$J \le x^{\mathrm{T}}(t_0)Px(t_0)\,. \tag{14}$$

Proof: Consider the following LKFs

$$V(t) = V_1(t) + V_2(t) + V_3(t) \tag{15}$$

where

$$V_1(t) = x^{\mathrm{T}}(t)Px(t) + \int_{t-\tau_U}^{t} x^{\mathrm{T}}(s)R_1x(s)\,\mathrm{d}s + \int_{t-\tau_L}^{t} x^{\mathrm{T}}(s)R_2x(s)\,\mathrm{d}$$

$$\begin{aligned}V_2(t) = &\int_{t-\tau(t)}^{t} x^{\mathrm{T}}(s)Qx(s)\,\mathrm{d}s \\ &+\big(\tau_U - \tau(t)\big)\eta^{\mathrm{T}}(t)\mathcal{X}\eta(t)\end{aligned}$$

$$V_3(t) = \int_{-\tau_U}^{-\tau_L}\int_{t+\theta}^{t} \dot{x}^{\mathrm{T}}(s)S\dot{x}(s)\,\mathrm{d}s\,\mathrm{d}\theta\,.$$

with

$$\Psi^{ij\tau_L} = \begin{bmatrix}
\pi_{11}^{ij\tau_L} & \pi_{12}^{ij\tau_L} & \pi_{13}^{ij\tau_L} & \pi_{14}^{ij\tau_L} & \pi_{15}^{ij\tau_L} & \pi_{16}^{ij\tau_L} & \pi_{17}^{ij} & \pi_{18}^{ij} & \sqrt{\tau^*}M_1^{\mathrm{T}} & \sqrt{3}J_1 & 0 & 0 \\
* & \pi_{22}^{ij\tau_L} & \pi_{23}^{ij} & \pi_{24}^{ij} & \pi_{25}^{ij\tau_L} & \pi_{26}^{ij\tau_L} & 0 & 0 & \sqrt{\tau^*}M_2^{\mathrm{T}} & K_j^{\mathrm{T}}J_2^{\mathrm{T}} & K_j^{\mathrm{T}}J_3^{\mathrm{T}} & J_3^{\mathrm{T}} \\
* & * & \pi_{33}^{ij} & \pi_{34}^{ij} & 0 & 0 & \pi_{37}^{ij\tau_L} & \pi_{38}^{ij\tau_L} & \sqrt{\tau^*}M_3^{\mathrm{T}} & 0 & 0 & 0 \\
* & * & * & \pi_{44}^{ij} & 0 & 0 & \pi_{47}^{ij\tau_L} & \pi_{48}^{ij\tau_L} & \sqrt{\tau^*}M_4^{\mathrm{T}} & 0 & 0 & 0 \\
* & * & * & * & \pi_{55}^{ij\tau_L} & \pi_{56}^{ij\tau_L} & \pi_{57}^{ij\tau_L} & \pi_{58}^{ij\tau_L} & 0 & 0 & 0 & 0 \\
* & * & * & * & * & \pi_{66}^{ij\tau_L} & 0 & 0 & 0 & K_j^{\mathrm{T}}J_2^{\mathrm{T}} & \sqrt{2}K_j^{\mathrm{T}}J_3^{\mathrm{T}} & 0 \\
* & * & * & * & * & * & \pi_{77}^{ij} & \pi_{78} & 0 & 0 & 0 & 0 \\
* & * & * & * & * & * & * & \pi_{88} & 0 & 0 & 0 & 0 \\
* & * & * & * & * & * & * & * & -S & 0 & 0 & 0 \\
* & * & * & * & * & * & * & * & * & -J_1 & 0 & 0 \\
* & * & * & * & * & * & * & * & * & * & -J_3 & 0 \\
* & * & * & * & * & * & * & * & * & * & 0 & -J_3
\end{bmatrix},$$

$$\mathcal{X} = \begin{bmatrix} X_1 + X_1^{\mathrm{T}} & -X_1 - X_2^{\mathrm{T}} & X_3 \\ * & X_2 + X_2^{\mathrm{T}} & X_4 \\ * & * & X_5 \end{bmatrix}$$

and $\eta^{\mathrm{T}}(t) = \left[x^{\mathrm{T}}(t)\ \int_{t-\tau_U}^{t-\tau(t)} x^{\mathrm{T}}(s)\,\mathrm{d}s\ \int_{t-\tau(t)}^{t-\tau_L} x^{\mathrm{T}}(s)\,\mathrm{d}s\right]$.

Now, estimating the time derivative of (15) with respect to the state trajectories of (10) will result as

$$\dot{V}(t) = \dot{V}_1(t) + \dot{V}_2(t) + \dot{V}_3(t)\,. \tag{16}$$

Here,

$$\begin{aligned}
\dot{V}_1(t) &= 2x^{\mathrm{T}}(t)P\dot{x}(t) + x^{\mathrm{T}}(t)(R_1 + R_2)x(t) \\
&\quad -x^{\mathrm{T}}(t-\tau_U)R_1x(t-\tau_U) - x^{\mathrm{T}}(t-\tau_L)R_2x(t-\tau_L), \\
\dot{V}_2(t) &= x^{\mathrm{T}}(t)Qx(t) \\
&\quad -\eta^{\mathrm{T}}(t)\mathcal{X}\eta(t) + 2[\tau_U - \tau(t)]\eta^{\mathrm{T}}(t)\mathcal{X}\dot{\eta}(t), \\
\dot{V}_3(t) &= (\tau_U - \tau_L)\dot{x}^{\mathrm{T}}(t)S\dot{x}(t) - \int_{t-\tau_U}^{t-\tau_L} \dot{x}^{\mathrm{T}}(s)S\dot{x}(s)\,\mathrm{d}s\,.
\end{aligned}$$

Also, the following integral term can be expressed into two integral terms

$$\begin{aligned}
-\int_{t-\tau_U}^{t-\tau_L} \dot{x}^{\mathrm{T}}(s)S\dot{x}(s)\,\mathrm{d}s &= -\int_{t-\tau_U}^{t-\tau(t)} \dot{x}^{\mathrm{T}}(s)S\dot{x}(s)\,\mathrm{d}s \\
&\quad -\int_{t-\tau(t)}^{t-\tau_L} \dot{x}^{\mathrm{T}}(s)S\dot{x}(s)\,\mathrm{d}s\,.
\end{aligned}$$

Consider the following zero equations for deriving the main results

$$\begin{aligned}
0 = 2\xi^{\mathrm{T}}(t)[M\ N]\Bigg(&\begin{bmatrix} x(t-\tau(t)) - x(t-\tau_U) \\ x(t-\tau_L) - x(t-\tau(t)) \end{bmatrix} \\
&-\begin{bmatrix} \int_{t-\tau_U}^{t-\tau(t)} \dot{x}(s)\,\mathrm{d}s \\ \int_{t-\tau(t)}^{t-\tau_L} \dot{x}(s)\,\mathrm{d}s \end{bmatrix}\Bigg).
\end{aligned} \tag{17}$$

In addition, one can express $S > 0$,

$$\begin{aligned}
-\begin{bmatrix} \int_{t-\tau_U}^{t-\tau(t)} \dot{x}^{\mathrm{T}}(s)S\dot{x}(s)\,\mathrm{d}s \\ \int_{t-\tau(t)}^{t-\tau_L} \dot{x}^{\mathrm{T}}(s)S\dot{x}(s)\,\mathrm{d}s \end{bmatrix} &\le 2\xi^{\mathrm{T}}(t)[M\ N] \\
&\quad \times \begin{bmatrix} x(t-\tau(t)) - x(t-\tau_U) \\ x(t-\tau_L) - x(t-\tau(t)) \end{bmatrix} \\
&\quad +\xi^{\mathrm{T}}(t)[M\ N]\tilde{S}_{\tau(t)}[M\ N]^{\mathrm{T}}\xi(t)
\end{aligned} \tag{18}$$

where

$\xi^{\mathrm{T}}(t) = [x^{\mathrm{T}}(t)\ x^{\mathrm{T}}(t-\tau(t))\ x^{\mathrm{T}}(t-\tau_U)\ x^{\mathrm{T}}(t-\tau_L)\,\dot{x}^{\mathrm{T}}(t)\ e^{\mathrm{T}}(i_kh) \int_{t-\tau_U}^{t-\tau(t)} x^{\mathrm{T}}(s)\,\mathrm{d}s\ \int_{t-\tau(t)}^{t-\tau_L} x^{\mathrm{T}}(s)\,\mathrm{d}s]$

$$\tilde{S}_{\tau(t)} = \begin{bmatrix} (\tau_U - \tau(t))S^{-1} & 0 \\ 0 & (\tau(t) - \tau_L)S^{-1} \end{bmatrix},$$

$M = [M_1^{\mathrm{T}}\, M_2^{\mathrm{T}}\, M_3^{\mathrm{T}}\, M_4^{\mathrm{T}}\, \underbrace{0 \ldots 0}_{4}]^{\mathrm{T}}$ and $N = [N_1^{\mathrm{T}}\, N_2^{\mathrm{T}}\, N_3^{\mathrm{T}}\, N_4^{\mathrm{T}}\, \underbrace{0 \ldots 0}_{4}]$.

From (10), we have

$$\begin{aligned}
\Omega_c = 2[&\alpha_c x^{\mathrm{T}}(t) + \beta_c x^{\mathrm{T}}(t-\tau(t)) + \gamma_c \dot{x}^{\mathrm{T}}(t) \\
&+\lambda_c e^{\mathrm{T}}(i_kh)]G\Big(-\dot{x}(t) + \sum_{i=1}^{p}\sum_{j=1}^{n_h} \omega_i(x(t))\hat{m}_j(x(t_kh)) \\
&\Big(A_ix(t) + B_iK_j\big[x(t-\tau(t)) - e(i_kh)\big]\Big),\ (c = 1, 2.)\,.
\end{aligned}$$

and

$$\frac{\tau_U - \tau(t)}{\tau_U - \tau_L}\Omega_1 + \frac{\tau(t) - \tau_L}{\tau_U - \tau_L}\Omega_2 = 0. \tag{19}$$

From the ET communication (4), for $t \in \left[i_kh + \tau_{t_k}, i_{k+1}h + \tau_{t_{k+1}}\right)$, it is clear that

$$\begin{aligned}
&-e^{\mathrm{T}}(i_kh)\Phi e(i_kh) \\
&\quad +\varepsilon\Big(x^{\mathrm{T}}(t-\tau(t)) - e^{\mathrm{T}}(i_kh)\Big)\Phi\Big(x(t-\tau(t)) - e(i_kh)\Big) \ge 0.
\end{aligned} \tag{20}$$

Moreover,

$$\begin{aligned}
u^{\mathrm{T}}(t)J_3u(t) &= \sum_{j=1}^{n_h} \hat{m}_j(x(t_kh))\big[x(t-\tau(t)) - e(i_kh)\big]^{\mathrm{T}}K_j^{\mathrm{T}}J_3 \\
&\quad \times \sum_{\varpi=1}^{n_h} m_\varpi(x(t_kh))K_\varpi\big[x(t-\tau(t)) - e(i_kh)\big], \\
&= \sum_{j=1}^{n_h}\sum_{\varpi=1}^{n_h} \hat{m}_j(x(t_kh))m_\varpi(x(t_kh))\big[x(t-\tau(t)) - e(i_kh)\big]^{\mathrm{T}}K_j^{\mathrm{T}} \\
&\quad \times J_3K_\varpi\big[x(t-\tau(t)) - e(i_kh)\big]\,.
\end{aligned}$$

Finally, (see (21)) . Based on the above,

$$\Psi^{ij\tau_U} = \begin{bmatrix}
\pi_{11}^{ij\tau_U} & \pi_{12}^{ij\tau_U} & \pi_{13}^{ij\tau_U} & \pi_{14}^{ij\tau_U} & \pi_{15}^{ij\tau_U} & \pi_{16}^{ij\tau_U} & \pi_{17}^{ij} & \pi_{18}^{ij} & \sqrt{\tau^*}N_1^{\mathrm{T}} & \sqrt{3}J_1 & 0 & 0 \\
* & \pi_{22}^{ij\tau_U} & \pi_{23}^{ij} & \pi_{24}^{ij} & \pi_{25\tau_U}^{ij} & \pi_{26}^{ij\tau_U} & 0 & 0 & \sqrt{\tau^*}N_2^{\mathrm{T}} & K_j^{\mathrm{T}}J_2^{\mathrm{T}} & K_j^{\mathrm{T}}J_3^{\mathrm{T}} & J_3^{\mathrm{T}} \\
* & * & \pi_{33}^{ij} & \pi_{34}^{ij} & 0 & 0 & \pi_{37}^{ij\tau_U} & \pi_{38}^{ij\tau_U} & \sqrt{\tau^*}N_3^{\mathrm{T}} & 0 & 0 & 0 \\
* & * & * & \pi_{44}^{ij} & 0 & 0 & \pi_{47}^{ij\tau_U} & \pi_{48}^{ij\tau_U} & \sqrt{\tau^*}N_4^{\mathrm{T}} & 0 & 0 & 0 \\
* & * & * & * & \pi_{55}^{ij\tau_U} & \pi_{56}^{ij\tau_U} & \pi_{57}^{ij\tau_U} & \pi_{58}^{ij\tau_U} & 0 & 0 & 0 & 0 \\
* & * & * & * & * & \pi_{66}^{ij\tau_U} & 0 & 0 & 0 & K_j^{\mathrm{T}}J_2^{\mathrm{T}} & \sqrt{2}K_j^{\mathrm{T}}J_3^{\mathrm{T}} & 0 \\
* & * & * & * & * & * & \pi_{77}^{ij} & \pi_{78} & 0 & 0 & 0 & 0 \\
* & * & * & * & * & * & * & \pi_{88} & 0 & 0 & 0 & 0 \\
* & * & * & * & * & * & * & * & -S & 0 & 0 & 0 \\
* & * & * & * & * & * & * & * & * & -J_1 & 0 & 0 \\
* & * & * & * & * & * & * & * & * & * & -J_3 & 0 \\
* & * & * & * & * & * & * & * & * & * & 0 & -J_3
\end{bmatrix}.$$

$$\begin{aligned}
&\begin{bmatrix} x(t) \\ u(t) \end{bmatrix}^{\mathrm{T}} \begin{bmatrix} J_1 & J_2 \\ * & J_3 \end{bmatrix} \begin{bmatrix} x(t) \\ u(t) \end{bmatrix} \le x^{\mathrm{T}}(t) J_1 x(t) \\
&\quad + 2x^{\mathrm{T}}(t) J_2 \sum_{j=1}^{n_h} \hat{m}_j(x(t_k h)) K_j \big[x(t-\tau(t)) - e(i_k h)\big] \\
&\quad + \sum_{j=1}^{n_h} \hat{m}_j(x(t_k h)) \big[x(t-\tau(t)) - e(i_k h)\big]^{\mathrm{T}} K_j^{\mathrm{T}} J_3 \\
&\quad \times K_j \big[x(t-\tau(t)) - e(i_k h)\big] \qquad (22) \\
&= \sum_{j=1}^{n_h} \hat{m}_j(x(t_k h)) \begin{bmatrix} x(t) \\ x(t-\tau(t)) \\ e(i_k h) \end{bmatrix}^{\mathrm{T}} \\
&\quad \times \begin{bmatrix} J_1 & J_2 K_j & -J_2 K_j \\ * & K_j^{\mathrm{T}} J_3 K_j & -K_j^{\mathrm{T}} J_3 K_j \\ * & * & K_j^{\mathrm{T}} J_3 K_j \end{bmatrix} \begin{bmatrix} x(t) \\ x(t-\tau(t)) \\ e(i_k h) \end{bmatrix}.
\end{aligned}$$

Based on Lemma 1, one can obtain,

$$\begin{aligned}
2x^{\mathrm{T}}(t)\, J_2 K_j x(t-\tau(t)) &\le x^{\mathrm{T}}(t) J_1 x(t) \\
&\quad + x^{\mathrm{T}}(t-\tau(t)) K_j^{\mathrm{T}} J_2^{\mathrm{T}} J_1^{-1} J_2 K_j x(t-\tau(t)) \\
-2x^{\mathrm{T}}(t)\, J_2 K_j e(i_k h) &\le x^{\mathrm{T}}(t) J_1 x(t) \\
&\quad + e^{\mathrm{T}}(i_k h) K_j^{\mathrm{T}} J_2^{\mathrm{T}} J_1^{-1} J_2 K_j e(i_k h) \qquad (23) \\
-2x^{\mathrm{T}}(t-\tau(t))\, K_j^{\mathrm{T}} J_3 K_j e(i_k h) &\le x^{\mathrm{T}}(t-\tau(t)) J_3 x(t-\tau(t)) \\
&\quad + e^{\mathrm{T}}(i_k h) K_j^{\mathrm{T}} J_3^{\mathrm{T}} J_3^{-1} J_3 K_j e(i_k h).
\end{aligned}$$

Now, rewrite the inequality (22) as follows

$$\begin{aligned}
&\begin{bmatrix} x(t) \\ u(t) \end{bmatrix}^{\mathrm{T}} \begin{bmatrix} J_1 & J_2 \\ * & J_3 \end{bmatrix} \begin{bmatrix} x(t) \\ u(t) \end{bmatrix} \le \sum_{j=1}^{n_h} \hat{m}_j(x(t_k h)) \big(3x^{\mathrm{T}}(t) J_1 x(t) \\
&\quad + x^{\mathrm{T}}(t-\tau(t)) \big(K_j^{\mathrm{T}} J_2^{\mathrm{T}} J_1^{-1} J_2 K_j + J_3 + K_j J_3 K_j^{\mathrm{T}} \big) \\
&\quad \times x(t-\tau(t)) + e^{\mathrm{T}}(i_k h) \big(K_j^{\mathrm{T}} J_2^{\mathrm{T}} J_1^{-1} J_2 K_j + K_j^{\mathrm{T}} J_3^{\mathrm{T}} J_3^{-1} J_3 K_j \\
&\quad + K_j^{\mathrm{T}} J_3 K_j \big) e(i_k h) \big).
\end{aligned}$$

Also,

$$\begin{aligned}
&\begin{bmatrix} x(t) \\ u(t) \end{bmatrix}^{\mathrm{T}} \begin{bmatrix} J_1 & J_2 \\ * & J_3 \end{bmatrix} \begin{bmatrix} x(t) \\ u(t) \end{bmatrix} \le \sum_{j=1}^{n_h} \hat{m}_j(x(t_k h)) \big(x^{\mathrm{T}}(t) (\sqrt{3} J_1) J_1^{-1} \\
&\quad \times (J_1^{\mathrm{T}} \sqrt{3}) x(t) + x^{\mathrm{T}}(t-\tau(t)) \big(K_j^{\mathrm{T}} J_2^{\mathrm{T}} J_1^{-1} J_2 K_j \\
&\quad + J_3^{\mathrm{T}} J_3^{-1} J_3 + (J_3 K_j)^{\mathrm{T}} J_3^{-1} (J_3 T K_j) \big) x(t-\tau(t)) \qquad (24) \\
&\quad + e^{\mathrm{T}}(i_k h) \big((J_2 K_j)^{\mathrm{T}} J_1^{-1} J_2 K_j \\
&\quad + (\sqrt{2} J_3 K_j)^{\mathrm{T}} J_3^{-1} (\sqrt{2} J_3 K_j) \big) e(i_k h) \big).
\end{aligned}$$

Here, we would like to mention J_1, J_2 are known matrices with appropriate dimension and J_3 is a positive scalar.

Adding (19) and (20) into (16), and from (24), we get

$$\begin{aligned}
&\dot{V}(t) + \begin{bmatrix} x(t) \\ u(t) \end{bmatrix}^{\mathrm{T}} \begin{bmatrix} J_1 & J_2 \\ * & J_3 \end{bmatrix} \begin{bmatrix} x(t) \\ u(t) \end{bmatrix} \\
&\le \sum_{i=1}^{p} \sum_{j=1}^{n_h} \omega_i(x(t)) \hat{m}_j(x(t_k h)) \xi^{\mathrm{T}}(t) \big(\Pi_{\tau(t)}^{ij} + (\tau_U - \tau(t)) M S^{-1} M^{\mathrm{T}} \qquad (25) \\
&\quad + (\tau(t) - \tau_L) N S^{-1} N^{\mathrm{T}} \big) \xi(t),
\end{aligned}$$

where

$$\Pi_{\tau(t)}^{ij} = \begin{bmatrix}
\bar{\pi}_{11}^{ij\tau(t)} & \pi_{12}^{ij\tau(t)} & \pi_{13}^{ij\tau(t)} & \pi_{14}^{ij\tau(t)} & \pi_{15}^{ij\tau(t)} & \pi_{16}^{ij\tau(t)} & \pi_{17}^{ij} & \pi_{18}^{ij} \\
* & \bar{\pi}_{22}^{ij\tau(t)} & \pi_{23}^{ij} & \pi_{24}^{ij} & \pi_{25}^{ij,\tau(t)} & \pi_{26}^{ij} & 0 & 0 \\
* & * & \pi_{33}^{ij} & \pi_{34}^{ij} & 0 & 0 & \pi_{37}^{ij\tau(t)} & \pi_{38}^{ij\tau(t)} \\
* & * & * & \pi_{44}^{ij} & 0 & 0 & \pi_{47}^{ij\tau(t)} & \pi_{48}^{ij\tau(t)} \\
* & * & * & * & \pi_{55}^{ij\tau(t)} & \pi_{56}^{ij\tau(t)} & \pi_{57}^{ij\tau(t)} & \pi_{58}^{ij\tau(t)} \\
* & * & * & * & * & \bar{\pi}_{66\tau(t)}^{ij} & 0 & 0 \\
* & * & * & * & * & * & \pi_{77}^{ij\tau(t)} & \pi_{78} \\
* & * & * & * & * & * & * & \pi_{88}
\end{bmatrix}$$

with

$$\begin{aligned}
\bar{\pi}_{11}^{ij\tau(t)} &= \pi_{11}^{ij\tau(t)} + (\sqrt{3} J_1) J_1^{-1} (J_1^{\mathrm{T}} \sqrt{3}), \\
\bar{\pi}_{22}^{ij\tau(t)} &= \pi_{22}^{ij\tau(t)} + (J_2 K_j)^{\mathrm{T}} J_1^{-1} J_2 K_j \\
&\quad + J_3 J_3^{-1} J_3 + (J_3 K_j)^{\mathrm{T}} J_3^{-1} K_j J_3, \\
\bar{\pi}_{66}^{ij\tau(t)} &= \bar{\pi}_{66}^{ij\tau(t)} + (J_2 K_j)^{\mathrm{T}} J_1^{-1} J_2 K_j + (\sqrt{2} J_3 K_j)^{\mathrm{T}} J_3^{-1} (\sqrt{2} K_j J_3).
\end{aligned}$$

Notice that, right side of (25) is convex combination of the terms $\Pi_{\tau(t)}^{ij}, (\tau_U - \tau(t)) M S^{-1} M^{\mathrm{T}}$ and $(\tau_U - \tau(t)) N S^{-1} N^{\mathrm{T}}$ with respect to $\tau(t) \in [\tau_L, \tau_U]$. Finally, we have derived the following LMIs

$$\Pi_{\tau_L}^{ij} + (\tau_U - \tau_L) M S^{-1} M^{\mathrm{T}} < 0, \qquad (26)$$

$$\Pi_{\tau_U}^{ij} + (\tau_U - \tau_L) N S^{-1} N^{\mathrm{T}} < 0. \qquad (27)$$

The above inequalities (26) and (27) is equivalent to (12) and (13) according to Schur complement lemma. From (12) and (13), one can conclude that

$$\dot{V}(t) + \begin{bmatrix} x(t) \\ u(t) \end{bmatrix}^{\mathrm{T}} \begin{bmatrix} J_1 & J_2 \\ * & J_3 \end{bmatrix} \begin{bmatrix} x(t) \\ u(t) \end{bmatrix} < 0. \qquad (28)$$

This implies that, system (10) is globally asymptotically stable. □

Remark 2: Theorem 1 contains a delay dependent based stability condition for ET-neural networks based control system. It should be mentioned that the proposed TDLF has the information of both lower and upper bounds of transmission delay $\tau(t)$. Also, the sufficient condition depends on some tuning parameters such as α_c, β_c, γ_c, λ_c in the zero-equation (19) and ϵ in (20). During the derivation of the feasible solutions, we will change the tuning parameter values by trial and error method until the better feasible stability region is reached, i.e. maximum bound of τ_U. Hence, the tuning parameters play a significant role in this work.

$$\begin{aligned}
u^{\mathrm{T}}(t) J_3 u(t) &\le \frac{1}{2} \sum_{j=1}^{n_h} \hat{m}_j(x(t_k h)) \big[x(t-\tau(t)) - e(i_k h)\big]^{\mathrm{T}} K_j^{\mathrm{T}} J_3 K_j \\
&\quad \times \big[x(t-\tau(t)) - e(i_k h)\big] + \frac{1}{2} \sum_{\varpi=1}^{n_h} m_{\varpi}(x(t_k h)) \big[x(t-\tau(t)) - e(i_k h)\big]^{\mathrm{T}} \\
&\quad \times K_{\varpi}^{\mathrm{T}} J_3 K_{\varpi} \big[x(t-\tau(t)) - e(i_k h)\big] \qquad (21) \\
&= \sum_{j=1}^{n_h} \hat{m}_j(x(t_k h)) \big[x(t-\tau(t)) - e(i_k h)\big]^{\mathrm{T}} \\
&\quad \times K_j^{\mathrm{T}} J_3 K_j \big[x(t-\tau(t)) - e(i_k h)\big].
\end{aligned}$$

Remark 3: The presence of $x(t-\tau(t))$ and $e(i_k h)$ in controller $u(t)$, the term $\begin{bmatrix} x(t) \\ u(t) \end{bmatrix}^{\mathrm{T}} \begin{bmatrix} J_1 & J_2 \\ * & J_3 \end{bmatrix} \begin{bmatrix} x(t) \\ u(t) \end{bmatrix}$ have turns into highly complex in terms of matrix inequalities. To solve such complexity, we utilised Lemma 1 and Schur complement lemma that can be represented as (22) in the proof of Theorem 1.

3.2 Control design

In this section, we will derive the stabilisation condition of the closed-loop (10) system based on Theorem 1. The outcomes of the derivations are summarised in the following theorem.

Theorem 2: For any given positive scalars τ_L, τ_U and any constants α_c, β_c, γ_c, λ_c $(c = 1, 2)$ and ϵ, the system (10) is said to be asymptotically stable, if there exist positive symmetric matrices $\hat{P}$, $\hat{R}_1$, $\hat{R}_2$, $\hat{S}$, $\hat{X}_5 \hat{Q} \in \mathbb{R}^{n \times n}$, and symmetric matrix $\hat{G}$, any matrices $\hat{X}_1$, $\hat{X}_2$, $\hat{X}_3$, $\hat{X}_4$, $\hat{M}_r$, $\hat{N}_r$, $(r = 1 \ldots 4)$ which satisfies the following LMIs $(i = 1, \ldots, p$ and $j = 1, \ldots, n_h)$

$$\hat{\Psi}^{ij\tau_L} < 0, \tag{29}$$

$$\hat{\Psi}^{ij\tau_U} < 0. \tag{30}$$

(see equation below)

All entries of $\hat{\Psi}^{ij\tau_L}$ and $\hat{\Psi}^{ij\tau_U}$ are given in Appendix 2.

Then, the proposed model (10) is said to be asymptotically stable with control gain matrices K_j calculated through

$$K_j = L_j \hat{G}^{-1} \tag{31}$$

and the corresponding value of the cost function (11) must satisfy the following inequality

$$J \leq x^{\mathrm{T}}(t_0) \hat{G}^{-T} \hat{P} \hat{G}^{-1} x(t_0).$$

Proof: Let $\hat{G} = G^{-1}$, $\hat{P} = \hat{G}^{\mathrm{T}} P \hat{G}$, $\hat{S} = \hat{G}^{\mathrm{T}} S \hat{G}$, $\hat{Q} = \hat{G}^{\mathrm{T}} Q \hat{G}$, $\hat{R} = \hat{G}^{\mathrm{T}} R_b \hat{G}\,(b = 1, \ldots, 6)$ $\hat{X}_5 = \hat{G}^{\mathrm{T}} X_5 \hat{G}$, $\hat{X}_1 = \hat{G}^{\mathrm{T}} X_1 \hat{G}$, $\hat{X}_2 = \hat{G}^{\mathrm{T}} X_2 \hat{G}$, $\hat{X}_3 = \hat{G}^{\mathrm{T}} X_3 \hat{G}$, $\hat{X}_4 = \hat{G}^{\mathrm{T}} X_4 \hat{G}$, $\hat{M}_c = \hat{G}^{\mathrm{T}} M_c \hat{G}$, $\hat{N}_c = \hat{G}^{\mathrm{T}} N_c \hat{G}$, $c = 1, \ldots 4.$, $\hat{\Phi} = \hat{G}^{\mathrm{T}} \Phi \hat{G}$ and $\coprod = \mathrm{diag}\{\hat{G}, \hat{G}, \hat{G}, \hat{G}, \hat{G}, \hat{G}, \hat{G}, \hat{G}, \hat{G}, \hat{G}, I, I, I\}$. Pre and post multiplying (12) and (13) by $\coprod^{\mathrm{T}}$ and $\coprod$, we can get the LMIs (29)–(30). □

Also, Theorem 2 proposes the sufficient condition with neural-network-based ET controller (9) and the cost function (11). Also, the proposed controller ensures that the closed-loop system is asymptotically stable. To find an optimal controller to minimise the upper bound of a given cost function. In this regard, we consider a scalar $\kappa > 0$ such that

$$x^{\mathrm{T}}(t_0) \hat{G}^{-1} \hat{P} \hat{G}^{-T} x(t_0) < \kappa. \tag{32}$$

The above inequality can be rewritten with Schur complement lemma as follows,

$$\begin{bmatrix} -\kappa & x^{\mathrm{T}}(t_0) \\ * & -\hat{G}^{\mathrm{T}} \hat{P}^{-1} \hat{G} \end{bmatrix} < 0. \tag{33}$$

Through utilising the condition $-\hat{G}^{\mathrm{T}} \hat{P}^{-1} \hat{G} \leq -\hat{G}^{\mathrm{T}} - \hat{G} + \hat{P}$, one can obtain that

$$\begin{bmatrix} -\kappa & x^{\mathrm{T}}(t_0) \\ * & -\hat{G}^{\mathrm{T}} - \hat{G} + \hat{P} \end{bmatrix} < 0. \tag{34}$$

From Theorem 2 and controller gain matrices K_j, the optimal value of cost function can be determined by solving the following optimisation problem

$$\hat{\Psi}^{ij\tau_L} = \begin{bmatrix}
\hat{\pi}_{11}^{ij\tau_L} & \hat{\pi}_{12}^{ij\tau_L} & \hat{\pi}_{13}^{ij\tau_L} & \hat{\pi}_{14}^{ij\tau_L} & \hat{\pi}_{15}^{ij\tau_L} & \hat{\pi}_{16}^{ij\tau_L} & \hat{\pi}_{17}^{ij} & \hat{\pi}_{18}^{ij} & \sqrt{\tau^*}\hat{M}_1^{\mathrm{T}} & \sqrt{3}\hat{G}J_1 & 0 & 0 \\
* & \hat{\pi}_{22}^{ij\tau_L} & \hat{\pi}_{23}^{ij} & \hat{\pi}_{24}^{ij} & \hat{\pi}_{25}^{ij\tau_L} & \hat{\pi}_{26}^{ij\tau_L} & 0 & 0 & \sqrt{\tau^*}\hat{M}_2^{\mathrm{T}} & L_j^{\mathrm{T}} J_2^{\mathrm{T}} & L_j^{\mathrm{T}} J_3^{\mathrm{T}} & \hat{G}J_3 \\
* & * & \hat{\pi}_{33}^{ij} & \hat{\pi}_{34}^{ij} & 0 & 0 & \hat{\pi}_{37}^{ij\tau_L} & \hat{\pi}_{38}^{ij\tau_L} & \sqrt{\tau^*}\hat{M}_3^{\mathrm{T}} & 0 & 0 & 0 \\
* & * & * & \hat{\pi}_{44}^{ij} & 0 & 0 & \hat{\pi}_{47}^{ij\tau_L} & \hat{\pi}_{48}^{ij\tau_L} & \sqrt{\tau^*}\hat{M}_4^{\mathrm{T}} & 0 & 0 & 0 \\
* & * & * & * & \hat{\pi}_{55}^{ij\tau_L} & \hat{\pi}_{56}^{ij\tau_L} & \hat{\pi}_{57}^{ij\tau_L} & \hat{\pi}_{58}^{ij\tau_L} & 0 & 0 & 0 & 0 \\
* & * & * & * & * & \hat{\pi}_{66}^{ij\tau_L} & 0 & 0 & 0 & L_j^{\mathrm{T}} J_2^{\mathrm{T}} & \sqrt{2} L_j^{\mathrm{T}} J_3^{\mathrm{T}} & 0 \\
* & * & * & * & * & * & \hat{\pi}_{77}^{ij} & \hat{\pi}_{78} & 0 & 0 & 0 & 0 \\
* & * & * & * & * & * & * & \hat{\pi}_{88} & 0 & 0 & 0 & 0 \\
* & * & * & * & * & * & * & * & -\hat{S} & 0 & 0 & 0 \\
* & * & * & * & * & * & * & * & * & -J_1 & 0 & 0 \\
* & * & * & * & * & * & * & * & * & * & -J_3 & 0 \\
* & * & * & * & * & * & * & * & * & * & 0 & -J_3 I_n
\end{bmatrix},$$

$$\hat{\Psi}^{ij\tau_U} = \begin{bmatrix}
\hat{\pi}_{11}^{ij\tau_U} & \hat{\pi}_{12}^{ij\tau_U} & \hat{\pi}_{13}^{ij\tau_U} & \hat{\pi}_{14}^{ij\tau_U} & \hat{\pi}_{15}^{ij\tau_U} & \hat{\pi}_{16}^{ij\tau_U} & \hat{\pi}_{17}^{ij} & \hat{\pi}_{18}^{ij} & \sqrt{\tau^*}\hat{N}_1^{\mathrm{T}} & \sqrt{3}\hat{G}J_1 & 0 & 0 \\
* & \hat{\pi}_{22}^{ij\tau_U} & \hat{\pi}_{23}^{ij} & \hat{\pi}_{24}^{ij} & \hat{\pi}_{25}^{ij\tau_U} & \hat{\pi}_{26}^{ij\tau_U} & 0 & 0 & \sqrt{\tau^*}\hat{N}_2^{\mathrm{T}} & L_j^{\mathrm{T}} J_2^{\mathrm{T}} & L_j^{\mathrm{T}} J_3^{\mathrm{T}} & \hat{G}J_3 \\
* & * & \hat{\pi}_{33}^{ij} & \hat{\pi}_{34}^{ij} & 0 & 0 & \hat{\pi}_{37}^{ij\tau_U} & \hat{\pi}_{38}^{ij\tau_U} & \sqrt{\tau^*}\hat{N}_3^{\mathrm{T}} & 0 & 0 & 0 \\
* & * & * & \hat{\pi}_{44}^{ij} & 0 & 0 & \hat{\pi}_{47}^{ij\tau_U} & \hat{\pi}_{48}^{ij\tau_U} & \sqrt{\tau^*}\hat{N}_4^{\mathrm{T}} & 0 & 0 & 0 \\
* & * & * & * & \hat{\pi}_{55}^{ij\tau_U} & \hat{\pi}_{56}^{ij\tau_U} & \hat{\pi}_{57}^{ij\tau_U} & \hat{\pi}_{58}^{ij\tau_U} & 0 & 0 & 0 & 0 \\
* & * & * & * & * & \hat{\pi}_{66}^{ij\tau_U} & 0 & 0 & 0 & L_j^{\mathrm{T}} J_2^{\mathrm{T}} & \sqrt{2} L_j^{\mathrm{T}} J_3^{\mathrm{T}} & 0 \\
* & * & * & * & * & * & \hat{\pi}_{77}^{ij} & \hat{\pi}_{78} & 0 & 0 & 0 & 0 \\
* & * & * & * & * & * & * & \hat{\pi}_{88} & 0 & 0 & 0 & 0 \\
* & * & * & * & * & * & * & * & -\hat{S} & 0 & 0 & 0 \\
* & * & * & * & * & * & * & * & * & -J_1 & 0 & 0 \\
* & * & * & * & * & * & * & * & * & * & -J_3 & 0 \\
* & * & * & * & * & * & * & * & * & * & 0 & -J_3 I_n
\end{bmatrix}.$$

Step		Optimal value of the cost function
1.	**Input**	Scalars τ_L, τ_U, α_c, β_c, γ_c, λ_c $(c = 1, 2)$ and ϵ, and given system matrices A_i and B_i
2	**if**	Optimization condition in (35) holds, **then**
3.		K_j are determined by $K_j = L_j\hat{G}^{-1}$
4.	**else**	
5.		**repeat** with optimal κ
6.	**end if**	
7.		N=0 to end time
8		Time step is 0.01
9.	**Input**	System parameters A_i, B_i, K_j and weight parameters $\hat{m}_{ij}$ and b_j
10.	**Input**	Initial value of states, i.e., $x(t_0)$.
11.	**for**	$i = 1$ to N **do**.
12		Solve model (10) via Euler method
13	**end**	

Fig. 3 *Algorithm 1: Finding the optimal value of the cost function*

Theorem 3: For any given positive scalars τ_L, τ_U and any constants α_c, β_c, γ_c, $\lambda_c\,(c = 1, 2)$ and ϵ, if the following optimisation problem

$$\begin{aligned} &\min J_{\min} = \kappa \\ &\text{subject to : (29)--(30), (34)} \\ &\qquad \hat{P} > 0,\ \hat{R}_1 > 0,\ \hat{R}_2 > 0,\ S,\ \hat{X}_5 > 0,\ \hat{Q} > 0, \\ &\qquad \hat{G}, \hat{M}_r,\ \hat{N}_r, (r = 1, \ldots, 4) \end{aligned} \tag{35}$$

has a solution $\hat{P} > 0,\ \hat{R}_1 > 0,\ \hat{R}_2 > 0,\ S,\ \hat{X}_5 > 0,\ \hat{Q} > 0,\ \hat{G},\ \hat{X}_1,\ \hat{X}_2,\ \hat{X}_3,\ \hat{X}_4,\ \hat{M}_r$ and $\hat{N}_r, (r = 1\ldots4)$, then $K_j = L_j\hat{G}^{-1}$ is the desired connection weights that ensure the optimal value of the cost function (11) for the system (10).

Remark 4: The main contribution of the present work is summarised as follows:

(i) An ET-TLFCFFNN based controller is designed to improve the stability performance of proposed (9).
(ii) The TDLF is introduced involving the information of lower and upper bound in the transmissions and also introduced some tuning parameters in the proposed sufficient conditions.
(iii) Optimise the cost function J^* in Theorem 3 that depends on $P, \hat{G}$ and initial conditions $x(t_0)$ and we can easily find the optimal value of κ by using Algorithm 1 (see Fig. 3).
(iv) Finally, the theoretical conditions will be validated with the help of WPGS models, that is, variable-speed wind turbine drive system, PMSM model. Besides that a inverted pendulum model will be considered (as a similar example of [11, 12] to show the less conservatism of the derived conditions.

In the following sections, we have been picturised the analysis of dynamical models, a variable-speed wind turbine drive system and PMSM model in terms of derived sufficient conditions provided in Theorems 1–3 on an individual manner. Finally, in order to prove the conservatism, an inverted pendulum model is conducted (as a similar example in [11, 12]) validated the sufficient conditions.

4 Applications

4.1 Modelling of variable-speed wind turbine drive system

In this section, we introduce the variable-speed wind turbine drive system and design a suitable control design with a three bladed horizontal-axis 60 KW wind turbine. The following state-space model of variable-speed wind turbine drive system was adapted from the works [29, 30].

$$\begin{aligned} Q_A - Q &= J_T\dot{\omega}_t, \\ Q - Q_E &= J_g\dot{\omega}_g, \\ Q = Q_s + Q_d &= K_s\int_0^t(\omega_t - \omega_g)\mathrm{d}t + B_s(\omega_t - \omega_g), \end{aligned} \tag{36}$$

where the description of parameters Q_{A}, Q_{E}, ω_{t}, ω_{g}, K_{s}, B_{s}, Q, J_{T} and J_g are discussed in the Nomenclature section

The power generation of the wind turbine is given by

$$P_{\mathrm{W}}(V, \lambda) = \frac{1}{2}\pi\rho\mathscr{R}^2C_{\mathrm{p}}(\lambda)V^3, \tag{37}$$

where C_{p}, the power coefficient of the turbine. The tip speed ratio λ, is given by

$$\lambda = \frac{\mathscr{R}\omega_{\mathrm{t}}}{V}. \tag{38}$$

In aerodynamics, variable torque coefficient function $C_{\mathrm{q}}(\lambda)$ has a significant role in the conversion of kinetic energy from the moving air into the mechanical torque Q_{A}. The $1-1$ corresponding power coefficient function is defined as $C_P(\lambda) = \lambda C_q(\lambda)$ and it is maximum power coefficient function is $C_P(\lambda)$. Moreover, the aerodynamic torque is given by

$$Q_{\mathrm{A}} = CC_q(\lambda), \tag{39}$$

where $C = \frac{1}{2}\rho A\mathscr{R}$, where A is the rotor disc area. Moreover, the generator torque is denoted by

$$Q_{\mathrm{E}} = \beta(\omega_g - \omega_s), \tag{40}$$

with ω_{s}, the synchronous speed. Now, we can rewrite the above model (36) into a state-space model with an assumption $\beta = 0$, as follows:

$$\begin{cases} \dot{x}_1 = & \frac{(\upsilon - B_{\mathrm{s}})}{J_{\mathrm{T}}}x_1 + \frac{B_{\mathrm{s}}}{J_{\mathrm{T}}}x_2 + \frac{1}{J_{\mathrm{T}}}x_3, \\ \dot{x}_2 = & \frac{B_{\mathrm{s}}}{J_{\mathrm{g}}}x_1 - \frac{B_{\mathrm{s}}}{J_{\mathrm{g}}}x_2 + \frac{1}{J_{\mathrm{g}}}x_3 - \frac{1}{J_{\mathrm{g}}}u, \\ \dot{x}_3 = & K_{\mathrm{s}}x_1 - K_{\mathrm{s}}x_2, \end{cases} \tag{41}$$

where $x = [x_1\, x_2\, x_3]^{\mathrm{T}} = [\omega_{\mathrm{t}}\, \omega_g\, Q_s]^{\mathrm{T}}$, $\upsilon = 0.5\rho A\mathscr{R}^3(C_p(\lambda_{\mathrm{opt}})/\lambda_{\mathrm{opt}}^2)x_1$ and $u = Q_R$. Here, the non-linear term Q_A is described as the convex combination of the valid operating points. In order to express it as linear model for (41), we assume that $x_1 \in [M_1\, M_2]$ with the following functions similar to result in [30]:

$$\omega_1(x(t)) = \frac{-x_1 + M_2}{M_2 - M_1}, \quad \omega_2(x(t)) = \frac{x_1 - M_1}{M_2 - M_1}. \tag{42}$$

The state-space model (41) can be described in terms of (42) as

$$\dot{x}(t) = \sum_{i=1}^{2}\omega_i(x(t))(A_ix(t) + B_iu(t)), \tag{43}$$

where

$$A_1 = \begin{bmatrix} \frac{\upsilon_1 - B_s}{J_T} & \frac{B_s}{J_T} & \frac{1}{J_T} \\ \frac{B_s}{J_g} & -\frac{B_s}{J_g} & \frac{1}{J_g} \\ K_s & -K_s & 0 \end{bmatrix},\ A_2 = \begin{bmatrix} \frac{\upsilon_2 - B_s}{J_T} & \frac{B_s}{J_T} & \frac{1}{J_T} \\ \frac{B_s}{J_g} & -\frac{B_s}{J_g} & \frac{1}{J_g} \\ K_s & -K_s & 0 \end{bmatrix},$$

$$B_1 = B_2 = \left[0\ -\frac{1}{J_g}\ 0\right]^{\mathrm{T}}.$$

From (5), the controller is given by

$$u(t) = \sum_{j=1}^{2} \hat{m}_j(x(t_k h))K_j x(t_k h),$$

where

$$t_f\Big(\sum_{i=1}^{3} m_{j,i}x_i(t_k h) - b_j\Big) = \frac{1}{1+\exp[-\sum_{i=1}^{3} m_{j,i}x_i(t_k h) - b_j]}.$$

4.1.1 Simulation results: This section contains the numerical simulation results in order to validate the effectiveness of the derived sufficient conditions (in Section 2). The parameter values of the proposed model (36) were extracted from Table 1.

The main task to find the largest value of τ_U based on the derived results (in Theorem 2) may ensure that the closed-loop system is asymptotically stable. Besides that, we choose $\alpha_1 = \beta_1 = \gamma_1 = \lambda_1 = \bar{c}_1$ with $\bar{c}_1 = 1.5$ and $\alpha_2 = \beta_2 = \gamma_2 = \lambda_2 = \bar{c}_2$, $\bar{c}_2 = 1.1$, $J_1 = \delta_1 I > 0$, $J_2 = [0\,0\,0]^{\mathrm{T}}$ and $J_3 = \delta_1 > 0$ where $\delta_1 \longrightarrow \infty$, the corresponding calculated maximum value of time-delay $\tau(t)$ is given in Table 2. Here, we would like to mention that, from Table 2, the value of δ_1 is inversely proportional to value of τ_U. For different matrix values of J_1 with $J_2 = [0\,0\,0]^{\mathrm{T}}$, $J_3 = 0.01$, $\bar{c}_1 = 1.5$ $\bar{c}_1 = 1.1$ and $\tau_L = 0.1$, the large upper bounds of the time-delay $\tau(t)$ and listed in the Table 3. Moreover, we have calculated the large upper bound values τ_U under different values of lower bound τ_L and $J_1 = I$, $J_2 = [0\,0\,0]^{\mathrm{T}}$, and $J_3 = 1.0$ (refer Table 4).

Now, let us consider the cost function value $\kappa = 150$, the upper bound value and lower bound value is assumed to be $\tau_L = 0.1$ and $\tau_U = 0.2$, respectively with $J_1 = \delta_1 I > 0$, $J_3 = \delta_1 > 0$ and $\delta_1 = 0.1$, $x(t_0) = [-2\,5\;-3]^{\mathrm{T}}$ and tuning parameters are fixed $\bar{c}_1 = 0.45$ and $\bar{c}_2 = 0.65$, the control gain matrices K_j are calculated from Theorem 3.

$$K_1 = [1.1244 \quad -2.9188 \quad 0.7384],$$
$$K_2 = [-0.8843 \quad -0.5207 \quad 0.1666]$$

Finally, we have chosen the weight parameters as $\hat{m}_{1,1} = -0.251$, $\hat{m}_{1,2} = -0.655$, $\hat{m}_{1,3} = -0.356$, $\hat{m}_{2,1} = -0.554$, $\hat{m}_{2,2} = -0.756$, $\hat{m}_{2,3} = -0.658$, $b_1 = -0.654$, $b_2 = -0.425$ and using the above gain matrices K_1 and K_2, the state trajectories of the model (43) shows the asymptotically stability behaviour under the proposed ET-neural-network-based controllers (9) in the Fig. 4. Fig. 5 depicts the response of the release instants and time intervals.

Table 1 The parameter values of the model

S.No.	Parameter	Value
1.	J_T	400,000 kg m^2
2.	J_G	65 kg m^2
3.	K_s	100 N ms/rad
4.	B_s	1800 N ms/rad
5.	R	35 m
6.	ρ	1.225 kg/m^3

Table 2 The large upper bound of $\tau(t)$ with $J_1 = \delta_1 I$, $J_2 = [0\,0\,0]^{\mathrm{T}}$, $J_3 = \delta_1$ and $\tau_L = 0.1$

δ_1	τ_U
10	0.2663
1	0.2736
0.1	0.2750
0.0001	0.2760

Table 3 The large upper bound of $\tau(t)$ with $J_2 = [0\,0\,0]$, $J_3 = 0.01$

τ_L	J_1	τ_U
0.1	$\begin{bmatrix}10&0&0\\0&1&0\\0&0&1\end{bmatrix}$	0.2747
0.1	$\begin{bmatrix}100&0&0\\0&1&0\\0&0&1\end{bmatrix}$	0.2720
0.1	$\begin{bmatrix}1000&0&0\\0&1&0\\0&0&1\end{bmatrix}$	0.2680

Table 4 The large upper bound of $\tau(t)$ with different values of lower bound τ_L

τ_L	τ_U
0	0.1821
0.1	0.2739
1	1.1516
10	10.0741

4.2 Modelling of non-linear permanent magnet synchronous motors

This section contains the investigation of the stabilisation for PMSM model through derived sufficient conditions. A lot of research works have been done on the analysis of dynamical behaviours becuase their non-linearities ([32–37]) and its compatibility with various industrial applications include wind energy conversion systems. To validate the derived sufficient conditons, we approximate the non-linear PMSM model (which is adapted from [33, 34]) with help of (3) and the obtained model is as follows

$$\begin{aligned} L_d\frac{\mathrm{d}i_d}{\mathrm{d}t} &= -R_s i_d + n_p\omega L_q i_q + u_d \\ L_d\frac{\mathrm{d}i_q}{\mathrm{d}t} &= -R_s i_q - n_p\omega L_d i_d - n_p\omega\Phi + u_q \\ J\frac{\mathrm{d}\omega}{\mathrm{d}t} &= n_p\big[(L_d - L_q)i_d i_q + \Phi i_q\big] - \beta\omega - T_L. \end{aligned} \tag{44}$$

We can get the following equations by using an affine transformation and time-scalling transformation as in [33, 35],

$$\begin{aligned} \dot{x}_1(t) &= -\frac{L_q}{L_d}x_1(t) + x_2(t)x_3(t) + \bar{u}_d \\ \dot{x}_2(t) &= -x_2(t) - x_1(t)x_3(t) + \bar{\gamma}x_3(t) + \bar{u}_q \\ \dot{x}_3(t) &= \bar{\sigma}(x_2(t) - x_3(t)) + \epsilon x_1(t)x_2(t) - \bar{T}_L \end{aligned} \tag{45}$$

with

$$\bar{\gamma} = \frac{n_p\Phi^2}{R_s\beta},\ \bar{\sigma} = \frac{L_q\beta}{R_s J},\ \bar{u}_q = \frac{n_p L_q\Phi u_q}{R_s^2\beta},$$
$$\bar{u}_d = \frac{n_p L_q\Phi u_d}{R_s^2\beta},\ \epsilon = \frac{L_q\beta^2(L_d - L_q)}{L_d J n_p\Phi^2},\ \bar{T}_L = \frac{L_q^2 T_L}{R_s^2 J},$$
$$n_p = 1,\ [x_1(t)\,x_2(t)\,x_3(t)]^{\mathrm{T}} = [i_d\,i_q\,\omega]^{\mathrm{T}}.$$

The descriptions of model is given in Table 5. If we assume the smooth-air-gap condition, i.e. $L_q = L_d$, the following equation will be obtained (see for more details, [35]) and the external inputs are assumed to be zero as $\bar{u}_d = \bar{u}_q = \bar{T}_L = 0$ in (45),

$$\begin{aligned} \dot{x}_1(t) &= -x_1(t) + x_2(t)x_3(t) \\ \dot{x}_2(t) &= -x_2(t) - x_1(t)x_3(t) + \bar{\gamma}x_3(t) \\ \dot{x}_3(t) &= \bar{\sigma}(x_2(t) - x_3(t)) \end{aligned} \tag{46}$$

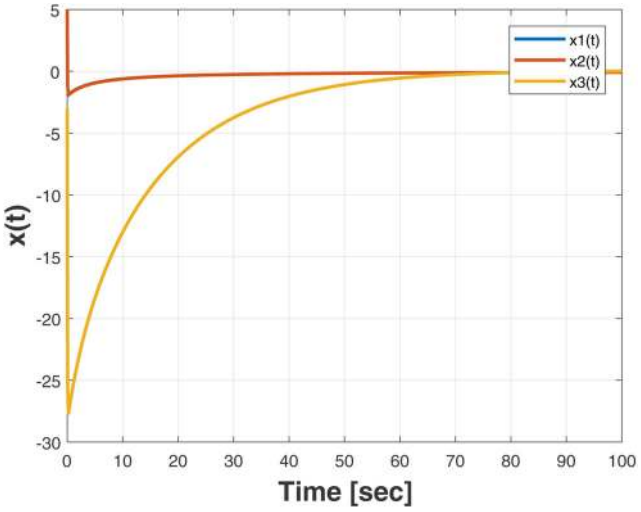

Fig. 4 *State response of the model (43) clearly shows that the state trajectories are congvergence to the origin for initial condition* $x(t_0) = [-2\ 5\ -3]^{\mathrm{T}}$

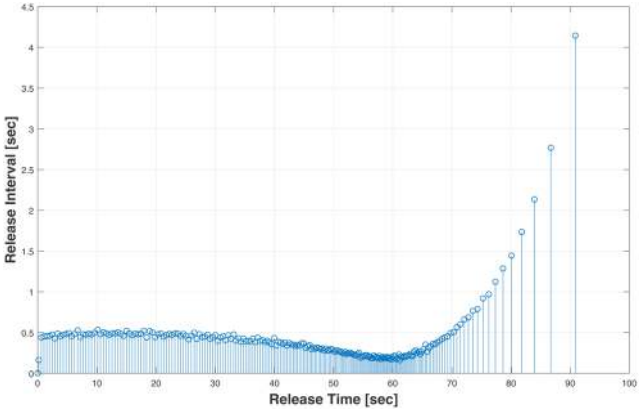

Fig. 5 *The response of release instants and release intervals based on proposed contoller is depicted*

Table 5 Description of model parameters (44)

Notations	Description
ω	rotor angular velocity
i_d and i_q	d–q axis currents
u_d and u_q	d–q axis voltages
R_s	Stator resistance
L_d and L_q	d–q axis stator inductors
n_p	pole pair
J	rotor moment of inertia
β	viscous friction coefficient
T_L	load torque
Φ	magnet flux linkage

Table 6 The large upper bound of $\tau(t)$ with $J_1 = \delta_1 I, J_2 = [0\,0\,0]^{\mathrm{T}}, J_3 = \delta_1$ and $\tau_L = 0.1$

δ_1	τ_U
10	0.3157
1	0.3157
0.1	0.3157
0.0001	0.3157

Here, $\bar{\gamma}$ and $\bar{\sigma}$ are positive constants. Kindly note the considered model (46) exhibits the chaotic solutions in nature. Hence, in order to stabilise the chaotic model, we have designed the controls for linear sub-models with help of (3) as,

$$\dot{x}(t) = \sum_{i=1}^{2} w_i(x_3(t))\big(A_i x(t) + B_i u(t)\big) \tag{47}$$

where

$$A_1 = \begin{bmatrix} -1 & \bar{d}_1 & 0 \\ -\bar{d}_1 & -1 & \bar{\gamma} \\ 0 & \bar{\sigma} & -\bar{\sigma} \end{bmatrix},\ A_2 = \begin{bmatrix} -1 & -\bar{d}_1 & 0 \\ \bar{d}_1 & -1 & \bar{\gamma} \\ 0 & \bar{\sigma} & -\bar{\sigma} \end{bmatrix},$$
$$B_1 = B_2 = \begin{bmatrix} 1 \\ 1 \\ 0 \end{bmatrix}.$$

and

$$w_1(x_3(t)) = \frac{1}{2}\Big(1 + \frac{x_3(t)}{\bar{d}_1}\Big),\ w_2(x_3(t)) = 1 - w_1(x_3(t)).$$

Moreover, from (5), the controller is given by

$$u(t) = \sum_{j=1}^{2} \hat{m}_j(x(t_k h))K_j x(t_k h),$$

where

$$t_f\Big(\sum_{i=1}^{3} \hat{m}_{j,i} x_i(t_k h) - b_j\Big) = \frac{1}{1 + \exp\big[-\sum_{i=1}^{3} \hat{m}_{j,i} x_i(t_k h) - b_j\big]}.$$

4.2.1 Simulation: The validation the PMSM model (47) under the proposed conditions along with the parameters values $\bar{\sigma} = 10$, $\bar{\gamma} = 1.1$, $\bar{d}_1 = 10$ are discussed in this section. Now, we start with the determination of largest value of τ_U that can be derived with Theorem 2 which guarantees the global asymptotic stability of the closed-loop system. Here, we assume $J_1 = \delta_1 I > 0$, $J_2 = [0\,0\,0]^{\mathrm{T}}$, $\bar{c}_1 = 0.80$, $\bar{c}_2 = 0.75$ and $J_3 = \delta_1 > 0$ where $\delta_1 \longrightarrow \infty$, and the corresponding large values of time-delay $\tau(t)$ are listed in Table 6. For different matrix values of J_1, $J_2 = [0\,0\,0]^{\mathrm{T}}$, $J_3 = 0.01$ and $\tau_L = 0.1$, the large upper bound of the time-delay $\tau(t)$ is listed in the Table 7. Moreover, we have also calculated the large upper bound value τ_U for different values of lower bound τ_L, $J_1 = I$, $J_2 = [0\,0\,0]^{\mathrm{T}}$, and $J_3 = 1.0$ and listed in Table 8.

Next, let us consider cost function value $\kappa = 50$ and the upper bound value and lower bound value are assumed to be $\tau_L = 0.0$ and $\tau_U = 0.01$, respectively. And also, $J_1 = \delta_1 I > 0$, $J_3 = \delta_1 > 0$, $\delta_1 = 0.1$, $x(t_0) = [20\,0.1\,5]^{\mathrm{T}}$ and tuning parameters are fixed as $\bar{c}_1 = 0.80$, $\bar{c}_2 = 0.75$ and finally the control gain matrices K_j are calculated via Theorem 3.

$$K_1 = [0.0035 \quad -0.0037 \quad 0.0294],$$
$$K_2 = [-0.0118 \quad -0.0180 \quad -0.0233].$$

We have chosen the weight parameter values as $\hat{m}_{1,1} = -2.56$, $\hat{m}_{1,2} = -1.55$, $\hat{m}_{1,3} = -2.634$, $\hat{m}_{2,1} = -0.124$,, $\hat{m}_{2,2} = -0.250$, $\hat{m}_{2,3} = -0.254$,, $b_1 = -0.8541$,, $b_2 = -0.92$ and with above gain matrices K_1, K_2, the state trajectories of the model (47) shows the asymptotic stability behaviour under the proposed ET-neural-network-based controllers (9) (see Fig. 6). In the Fig. 7, the response of the release instants and time intervals are depicted.

5 A comparison example

In the previous two sections, we have validated the derived sufficient conditions with variable-speed wind turbine drive system

Table 7 The large upper bound of $\tau(t)$ with $J_2 = [0\,0\,0]$, $J_3 = 0.01$

τ_L	J_1	τ_U
0.1	$\begin{bmatrix}10 & 0 & 0\\ 0 & 1 & 0\\ 0 & 0 & 1\end{bmatrix}$	0.3157
0.1	$\begin{bmatrix}100 & 0 & 0\\ 0 & 1 & 0\\ 0 & 0 & 1\end{bmatrix}$	0.3154
0.1	$\begin{bmatrix}1000 & 0 & 0\\ 0 & 1 & 0\\ 0 & 0 & 1\end{bmatrix}$	0.3145

Table 8 The large upper bound of $\tau(t)$ with different value of lower bound τ_L

τ_L	τ_U
0	0.2242
0.1	0.3157
1	1.1743
10	10.0737

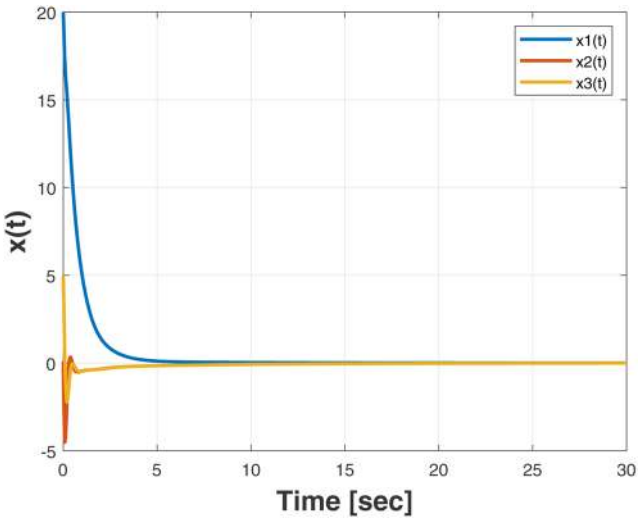

Fig. 6 *State response of the model (47) and it clearly shows that the state trajectories are converged to the origin for initial conditions* $[20\ 0.1\ -5]^{\mathrm{T}}$

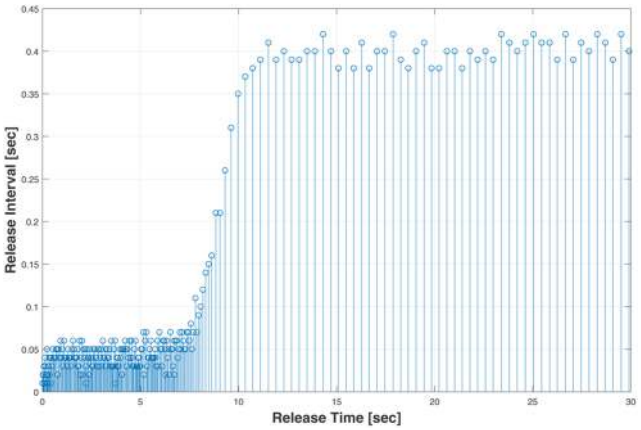

Fig. 7 *Shows the response of release instants and release intervals based on proposed controller*

and PMSM models. In order to prove the conservatism of the derived conditions, we have considered an inverted pendulum model as in [11, 12].

$$\ddot{\theta}(t) = \frac{g\sin(\theta(t)) - am_pL\dot{\theta}^2(t)\frac{\sin(2\theta(t))}{2} - a\cos(\theta(t))u(t)}{\frac{4L}{3} - am_pL\cos^2(\theta(t))} \tag{48}$$

here $\theta(t)$ is angular displacement of the pendulum and $g = 9.8m/s^2$ denotes the acceleration of gravity, $m_p \in [2, 5]$ kg is the mass of the pendulum, $M_c \in [M_{c\min}, M_{c\max}] = [30, 35]$ kg is the mass of the cart. $2L = 1$ m is the length of the pendulum. $u(t)$ denotes force input. m_p, and M_c are regarded the parameter uncertainties. $a = 1/(m_p + M_c)$. The inverted pendulum can be expressed as dynamical equations by letting $[x_1^{\mathrm{T}}(t)\, x_2^{\mathrm{T}}(t)]^{\mathrm{T}} = [\theta^{\mathrm{T}}(t)\, \dot{\theta}^{\mathrm{T}}(t)]^{\mathrm{T}}$ as given below

$$\dot{x}(t) = \sum_{i=1}^{4} \omega_i(x(t))(A_ix(t) + B_iu(t)), \tag{49}$$

where $x_1(t) \in [x_{1\min}, x_{1\max}] = [-\pi/3, \pi/3]$ and $x_2(t) \in [x_{2\min}, x_{2\max}] = [-5, 5]$. The remaining parameters are chosen as in [11, 12],

$$A_1 = A_2 = \begin{bmatrix}0 & 1\\ f_{1\min} & 0\end{bmatrix},\ A_3 = A_4 = \begin{bmatrix}0 & 1\\ f_{1\max} & 0\end{bmatrix},$$
$$B_1 = B_3 = \begin{bmatrix}0\\ f_{2\min}\end{bmatrix},\quad B_2 = B_4 = \begin{bmatrix}0\\ f_{2\max}\end{bmatrix}.$$

and

$$\omega_i(x(t)) = \frac{\mu_i(f_1(x(t)) \times v_i(f_2(x(t))}{\sum_{j=1}^{4}\left(\mu_j(f_1(x(t)) \times v_j(f_2(x(t)))\right)}$$

in which $f_{1\min} = 11.3533$, $f_{1\max} = 16.4640$, $f_{2\min} = -0.0192$, $f_{1\max} = -0.0492$ and

$$\mu_j(f_1(x(t))) = \frac{-f_1(x(t) + f_{1\max}}{f_{1\max} - f_{1\min}},\ j = 1, 2$$
$$\mu_j(f_1(x(t))) = 1 - \mu_1(f_1(x(t))),\ j = 3, 4$$
$$v_j(f_2(x(t))) = \frac{-f_2(x(t) + f_{2\max}}{f_{2\max} - f_{2\min}},\ j = 1, 3$$
$$v_j(f_2(x(t))) = 1 - v_1(f_2(x(t))),\ j = 2, 4$$
$$f_1(x(t)) = \frac{g - am_pLx_2^2(t)\cos(x(t))}{4L/3 - am_pL\cos^2(x_1(t))}\left(\frac{\sin(x_1(t))}{x_1(t)}\right)$$
$$f_2(x(t)) = \frac{a\cos(x(t))}{4L/3 - am_pL\cos^2(x_1(t))}.$$

Moreover, we have proposed an ET-neural network-based controller in the form of (5) with four hidden nodes is used to stabilise the model (49), which is given by

$$u(t) = \sum_{j=1}^{4} \hat{m}_j(x(t_kh))K_jx(t_kh), \tag{50}$$

where

$$t_f\left(\sum_{i=1}^{2}\hat{m}_{j,i}x_i(t_kh) - b_j\right) = \frac{1}{1 + \exp\left[-\sum_{i=1}^{3}\hat{m}_{j,i}x_i(t_kh) - b_j\right]}.$$

with the corresponding parameter values are

$$\hat{m}_{1,1} = -0.0591,\ \hat{m}_{1,2} = 0.5511,\ \hat{m}_{2,1} = -0.9863,\ \hat{m}_{2,2} = 0.5118,$$
$$\hat{m}_{3,1} = 0.3058,\ \hat{m}_{3,2} = 0.1582,\ \hat{m}_{4,1} = -0.6254,\ \hat{m}_{4,2} = -0.7569,$$
$$b_1 = -0.2765,\ b_2 = -0.3234,\ b_3 = -0.7899,\ b_4 = 0.4423,$$

and $m_p = 2$ kg, $M_c = 30$ kg. The authors in [11, 12] have been validated the model (49) with same parameter values under the SDNNC. However, in this paper, we have validate the sufficient

Table 9 Large upper bound

Method	τ_U
Theorem 1 in [11]	0.0662
Theorem 1 in [12]	0.1093
Theorem 2 in [28]	0.1285
Theorem 2 ($\tau_L = 0$)	0.2401
Theorem 2 ($\tau_L = 0.5$)	0.6684
Theorem 2 ($\tau_L = 1$)	1.1419

condition with the proposed model (49) under the ET-Neural Network-based controller (50). For the comparison results, let use chose the same parameter values i.e. $J_1 = \delta_1 I > 0$, $J_2 = [0\,0]^{\mathrm{T}}$, and $J_3 = \delta_1 = 10^{-6}$ as in [11, 12]. The solving the LMIs in Theorem 2 with triggered parameters $\epsilon = 1$ and tuning parameters are chosen $\alpha_1 = \beta_1 = \gamma_1 = \lambda_1 = \bar{c}_1$ with $\bar{c}_1 = 0.25$ and $\alpha_2 = \beta_2 = \gamma_2 = \lambda_2 = \bar{c}_2$, $\bar{c}_2 = 0.35$, the maximum upper bound τ_U is calculated, which are listed in the Table 9. From the table, we can conclude that the derived sufficient conditions can produce a large upper bound than existing works.

Next, let us consider cost function value $\kappa = 25.50$ and the upper bound value and lower bound value are assumed to be $\tau_L = 0.0$ and $\tau_U = 0.2$, respectively. And also, $J_1 = \delta_1 I > 0$, $J_3 = \delta_1 > 0$, $\delta_1 = 0.1$, $x(t_0) = [\pi/6\,0]^{\mathrm{T}}$ and tuning parameters are fixed as $\bar{c}_1 = 0.25$, $\bar{c}_2 = 0.35$ and finally the control gain matrices K_j are calculated via Theorem 3.

$$K_1 = [-0.0105 \quad 0.0237],\ K_2 = [-0.0105 \quad 0.0237].$$

Here, it should be mentioned that the state response of the simulation results is omitted due to the reduced number of pages. Form this example, it is clearly observed that the derived sufficient conditions give significantly improved results than existing works [11, 12, 28].

6 Conclusion

The paper dealt with the stabilisation problem for an ET-Neural Network-based control system and its direct application to variable-speed wind turbine drive system, PMSM and inverted pendulum model. The novel controller is designed under the ET scheme for TLFCFFNN. Based on suitable TDLF and performance cost function, some novel stability and stabilisation criteria have formulated in terms of solvable LMIs. The control gain matrices K_j have been calculated through the derived sufficient conditions which result in the global asymptotic stable performance of the closed-loop system. To validate the conditions, these non-linear models are taken into the analysis and their corresponding feasibility is guaranteed with the proposed LMIs. The numerical results support the effectiveness and show the merit of the derived conditions. For further improvement of this study, we will focus on how to validate the presented models with experimental data and the corresponding results will be summarised in the future.

7 Acknowledgments

This work was supported by the Korea Research Fellowship Program through the National Research Foundation of Korea (NRF) funded by the Ministry of Science and ICT (KRF project grant number 2017H1D3A1A01014107) and by the Basic Science Research Program through the NRF funded by the Ministry of Education (NRF-2016R1A6A1A03013567, NRF-2018R1A2A2A14023632).

8 References

[1] Bianchi, F.D., Mantz, R.J., De Battista, H.: 'The wind and wind turbines', '*Wind Turbine Control Systems: Principles, modelling and gain scheduling design*' (Springer, 2007), pp. 7–28

[2] Kazachkov, Y., Feltes, J.W., Zavadil, R.: 'Modeling wind farms for power system stability studies'. Power Engineering Society General Meeting, Toronto, Ontario, Canada, 2003, vol. 3, pp. 1526–1533

[3] Baloch, M.H., Wang, J., Kaloi, G.S.: 'Stability and nonlinear controller analysis of wind energy conversion system with random wind speed', *Int. J. Electr. Power Energy Syst.*, 2016, **79**, pp. 75–83

[4] Kamal, E., Aitouche, A., Ghorbani, R., *et al.*: 'Robust nonlinear control of wind energy conversion systems', *Int. J. Electr. Power Energy Syst.*, 2013, **44**, (1), pp. 202–209

[5] Yang, B., Yu, T., Shu, H., *et al.*: 'Robust sliding-mode control of wind energy conversion systems for optimal power extraction via nonlinear perturbation observers', *Appl. Energy*, 2018, **210**, pp. 711–723

[6] Schulte, H., Gauterin, E.: 'Input-to-state stability condition for passive fault-tolerant control of wave and wind energy converters', *IFAC-PapersOnLine*, 2015, **48**, (21), pp. 257–262

[7] Schulte, H., Gauterin, E.: 'Fault-tolerant control of wind turbines with hydrostatic transmission using Takagi–Sugeno and sliding mode techniques', *Annual Rev. Control*, 2015, **40**, pp. 82–92

[8] Gnaneswaran, N., Joo, Y.H.: 'Event-triggered stabilization for T-S fuzzy systems with asynchronous premise constraints and its application to wind turbine system', *IET Control Theory Applic.*, 2019, **13**, (10), pp. 1532–1542

[9] Wang, T., Gao, H., Qiu, J.: 'A combined adaptive neural network and nonlinear model predictive control for multirate networked industrial process control', *IEEE Trans. Neural Netw. Learn. Syst.*, 2016, **27**, (2), pp. 416–425

[10] Li, Y.-X., Yang, G.-H.: 'Adaptive neural control of pure-feedback nonlinear systems with event-triggered communications', *IEEE Trans. Neural Netw. Learn. Syst.*, 2018, **29**, (12), pp. 6242–6251

[11] Lam, H., Leung, F.H.: 'Design and stabilization of sampled-data neural-network-based control systems', *IEEE Trans. Syst. Man Cybern., B, Cybern.*, 2006, **36**, (5), pp. 995–1005

[12] Zhu, X.-L., Wang, Y.: 'Stabilization for sampled-data neural-network-based control systems', *IEEE Trans. Syst. Man Cybern., B, Cybern.*, 2011, **41**, (1), pp. 210–221

[13] Wu, Z.-G., Shi, P., Su, H., *et al.*: 'Exponential stabilization for sampled-data neural-network-based control systems', *IEEE Trans. Neural Netw. Learn. Syst.*, 2014, **25**, (12), pp. 2180–2190

[14] Wang, Y., Shen, H., Duan, D.: 'On stabilization of quantized sampled-data neural-network-based control systems', *IEEE Trans. Cybern.*, 2017, **47**, (10), pp. 3124–3135

[15] Åström, K.J., Wittenmark, B.: '*Computer-controlled systems: theory and design*' (Courier Corporation, New York, USA, 2013)

[16] Chen, T., Francis, B.A.: '*Optimal sampled-data control systems*' (Springer Science & Business Media, London, 2012)

[17] Ding, L., Han, Q.-L., Ge, X., *et al.*: 'An overview of recent advances in event-triggered consensus of multiagent systems', *IEEE Trans. Cybern.*, 2018, **48**, (4), pp. 1110–1123

[18] Li, Q., Shen, B., Wang, Z., *et al.*: 'Synchronization control for a class of discrete time-delay complex dynamical networks: a dynamic event-triggered approach', *IEEE Trans. Cybern.*, 2019, **49**, (5), pp. 1979–1986

[19] Wang, X.L., Yang, G.H.: 'Event-triggered H^{∞} filtering for discrete-time T–S fuzzy systems via network delay optimization technique', *IEEE Trans. Syst. Man Cybern., Syst.*, 2019, **49**, (10), pp. 2026–2035

[20] Yue, D., Tian, E., Han, Q.-L.: 'A delay system method for designing event-triggered controllers of networked control systems', *IEEE Trans. Autom. Control*, 2013, **58**, (2), pp. 475–481

[21] Peng, C., Ma, S., Xie, X.: 'Observer-based non-PDC control for networked T–S fuzzy systems with an event-triggered communication', *IEEE Trans. Cybern.*, 2017, **47**, (8), pp. 2279–2287

[22] Peng, C., Yang, T.C.: 'Event-triggered communication and H_{∞} control co-design for networked control systems', *Automatica*, 2013, **49**, (5), pp. 1326–1332

[23] Li, H., Chen, Z., Wu, L., *et al.*: 'Event-triggered fault detection of nonlinear networked systems', *IEEE Trans. Cybern.*, 2017, **47**, (4), pp. 1041–1052

[24] Meng, X., Chen, T.: 'Event triggered robust filter design for discrete-time systems', *IET Control Theory Applic.*, 2014, **8**, (2), pp. 104–113

[25] Yu, H., Hao, F.: 'Design of event conditions in event-triggered control systems: a non-fragile control system approach', *IET Control Theory Applic.*, 2016, **10**, (9), pp. 1069–1077

[26] Tarbouriech, S., Seuret, A., da Silva, J.M.G.Jr., *et al.*: 'Observer-based event-triggered control co-design for linear systems', *IET Control Theory Applic.*, 2016, **10**, (18), pp. 2466–2473

[27] Shen, H., Li, F., Yan, H., *et al.*: 'Finite-time event-triggered H_{∞} control for T-S fuzzy markov jump systems', *IEEE Trans. Fuzzy Syst.*, 2018, **26**, (5), pp. 3122–3135

[28] Hu, S., Yue, D., Xie, X., *et al.*: 'Stabilization of neural-network-based control systems via event-triggered control with nonperiodic sampled data', *IEEE Trans. Neural Netw. Learn. Syst.*, 2016, **29**, (3), pp. 573–585

[29] Novak, P., Ekelund, T., Jovik, I., *et al.*: 'Modeling and control of variable-speed wind-turbine drive-system dynamics', *IEEE Control Syst.*, 1995, **15**, (4), pp. 28–38

[30] Sung, H.C., Park, J.B., Joo, Y.H.: 'Robust observer-based fuzzy control for variable speed wind power system: LMI approach', *Int. J. Control Autom. Syst.*, 2011, **9**, (6), pp. 1103–1110

[31] Thuan, M.V., Phat, V.N.: 'Optimal guaranteed cost control of linear systems with mixed interval time-varying delayed state and control', *J. Optim. Theory Appl.*, 2012, **152**, (2), pp. 394–412

[32] Li, Z., Park, J.B., Joo, Y.H., *et al.*: 'Bifurcations and chaos in a permanent-magnet synchronous motor', *IEEE Trans. Circuits Syst. I, Fundam. Theory Appl.*, 2002, **49**, (3), pp. 383–387

[33] Jing, Z., Yu, C., Chen, G.: 'Complex dynamics in a permanent-magnet synchronous motor model', *Chaos, Solitons & Fractals*, 2004, **22**, (4), pp. 831–848

[34] Zhang, F., Liao, X., Mu, C.: 'Dynamical analysis of the permanent-magnet synchronous motor chaotic system', *Adv. Differ. Equ.*, 2017, **2017**, (1), p. 76

[35] Chen, Q., Ren, X., Na, J.: 'Robust finite-time chaos synchronization of uncertain permanent magnet synchronous motors', *ISA Trans.*, 2015, **58**, pp. 262–269
[36] Shanmugam, L., Joo, Y.H.: 'Design of interval type-2 fuzzy-based sampled-data controller for nonlinear systems using novel fuzzy Lyapunov functional and its application to PMSM', *IEEE Trans. Syst. Man Cybern., Syst.*, 2018, pp. 1–10, DOI: 10.1109/TSMC.2018.2875098
[37] Mani, P., Rajan, R., Shanmugam, L., *et al.*: 'Adaptive fractional fuzzy integral sliding mode control for PMSM model', *IEEE Trans. Fuzzy Syst.*, 2019, **27**, (8), pp. 1674–1686

9 Appendix

9.1 Appendix 1

For $\tau(t) = \tau_L, \tau(t) = \tau_U$ as in the following terms, we can get the terms of $\Psi^{ij\tau_L}$ and $\Psi^{ij\tau_U}$.

(see equation below)

9.2 Appendix 2

For $\tau(t) = \tau_L, \tau(t) = \tau_U$ as in the following terms, we can get the terms of $\hat{\Psi}^{ij\tau_L}$ and $\hat{\Psi}^{ij\tau_U}$.

(see equation below)

$$\pi_{11}^{ij\tau(t)} = -(X_1 + X_1^T) + \Big(\frac{\tau_U - \tau(t)}{\tau_U - \tau_L}\alpha_1 + \frac{\tau(t) - \tau_L}{\tau_U - \tau_L}\alpha_2\Big)(GA_i + A_i^T G^T) + Q + R_1 + R_2,$$

$$\pi_{12}^{ij\tau(t)} = \Big(\frac{\tau_U - \tau(t)}{\tau_U - \tau_L}\beta_1 + \frac{\tau(t) - \tau_L}{\tau_U - \tau_L}\beta_2\Big) \times A_i^T G^T + \Big(\frac{\tau_U - \tau(t)}{\tau_U - \tau_L}\alpha_1 + \frac{\tau(t) - \tau_L}{\tau_U - \tau_L}\alpha_2\Big)GB_iK_j + M_1 - N_1,$$

$$\pi_{13}^{ij\tau(t)} = (\tau_U - \tau(t))(X_1 + X_2^T) - M_1, \quad \pi_{14}^{ij\tau(t)} = (\tau_U - \tau(t))X_3 + N_1,$$

$$\pi_{15}^{ij\tau(t)} = P - \Big(\frac{\tau_U - \tau(t)}{\tau_U - \tau_L}\alpha_1 + \frac{\tau(t) - \tau_L}{\tau_U - \tau_L}\alpha_2\Big)G + \Big(\frac{\tau_U - \tau(t)}{\tau_U - \tau_L}\gamma_1 + \frac{\tau(t) - \tau_L}{\tau_U - \tau_L}\gamma_2\Big)A_i^T G^T + (\tau_U - \tau(t))(X_1 + X_1^T),$$

$$\pi_{16}^{ij\tau(t)} = \Big(\frac{\tau_U - \tau(t)}{\tau_U - \tau_L}\lambda_1 + \frac{\tau(t) - \tau_L}{\tau_U - \tau_L}\lambda_2\Big)A_i^T G^T - \Big(\frac{\tau_U - \tau(t)}{\tau_U - \tau_L}\alpha_1 + \frac{\tau(t) - \tau_L}{\tau_U - \tau_L}\alpha_2\Big)GB_iK_j, \ \pi_{17}^{ij} = X_1 + X_2^T, \ \pi_{18}^{ij} = -X_3,$$

$$\pi_{22}^{ij\tau(t)} = M_2 + M_2^T - N_2 - N_2^T + 2\Big(\frac{\tau_U - \tau(t)}{\tau_U - \tau_L}\beta_1 + \frac{\tau(t) - \tau_L}{\tau_U - \tau_L}\beta_2\Big)GB_iK_j + \epsilon\Phi,$$

$$\pi_{23}^{ij} = -M_2 + M_3^T - N_3^T, \quad \pi_{24}^{ij} = N_2 - N_4^T + M_4^T,$$

$$\pi_{25}^{ij\tau(t)} = -\Big(\frac{\tau_U - \tau(t)}{\tau_U - \tau_L}\beta_1 + \frac{\tau(t) - \tau_L}{\tau_U - \tau_L}\beta_2\Big)G + \Big(\frac{\tau_U - \tau(t)}{\tau_U - \tau_L}\gamma_1 + \frac{\tau(t) - \tau_L}{\tau_U - \tau_L}\gamma_2\Big)K_j^T Bi^T G^T,$$

$$\pi_{26}^{ij\tau(t)} = -\Big(\frac{\tau_U - \tau(t)}{\tau_U - \tau_L}\beta_1 + \frac{\tau(t) - \tau_L}{\tau_U - \tau_L}\beta_2\Big)GB_iK_j + \Big(\frac{\tau_U - \tau(t)}{\tau_U - \tau_L}\lambda_1 + \frac{\tau(t) - \tau_L}{\tau_U - \tau_L}\lambda_2\Big)K_j^T Bi^T G^T - \epsilon\Phi,$$

$$\pi_{33}^{ij} = -R_1 - M_3 - M_3^T, \ \pi_{34}^{ij} = -M_4^T + N_3, \quad \pi_{37}^{ij\tau(t)} = -(\tau_U - \tau(t))(X_2 + X_2^T),$$

$$\pi_{38}^{ij\tau(t)} = -(\tau_U - \tau(t))X_4, \quad \pi_{44}^{ij} = -R_2 + N_4 + N_4^T,$$

$$\pi_{47}^{ij\tau(t)} = (\tau_U - \tau(t))X_4, \quad \pi_{48}^{ij\tau(t)} = (\tau_U - \tau(t))X_5, \quad \pi_{55}^{ij\tau(t)} = -\Big(\frac{\tau_U - \tau(t)}{\tau_U - \tau_L}\gamma_1 + \frac{\tau(t) - \tau_L}{\tau_U - \tau_L}\gamma_2\Big)(G + G^T) + \tau^* S,$$

$$\pi_{56}^{ij\tau(t)} = -\Big(\frac{\tau_U - \tau(t)}{\tau_U - \tau_L}\lambda_1 + \frac{\tau(t) - \tau_L}{\tau_U - \tau_L}\lambda_2\Big)G^T - \Big(\frac{\tau_U - \tau(t)}{\tau_U - \tau_L}\gamma_1 + \frac{\tau(t) - \tau_L}{\tau_U - \tau_L}\gamma_2\Big)GB_iK_j,$$

$$\pi_{57}^{ij\tau(t)} = -(\tau_U - \tau(t))(X_1^T + X_2), \quad \pi_{58}^{ij\tau(t)} = (\tau_U - \tau(t))X_3,$$

$$\pi_{66}^{ij\tau(t)} = -\Big(\frac{\tau_U - \tau(t)}{\tau_U - \tau_L}\lambda_1 + \frac{\tau(t) - \tau_L}{\tau_U - \tau_L}\lambda_2\Big)(G + G^T) + (\epsilon - 1)\Phi, \quad \pi_{77}^{ij} = -(X_2 + X_2^T),$$

$$\pi_{78}^{ij} = -X_4, \quad \pi_{88}^{ij} = -X_5 \text{ and } \tau^* = \tau_U - \tau_L.$$

$$\hat{\pi}_{11}^{ij\tau(t)} = -(\hat{X}_1 + \hat{X}_1^T) + \Big(\frac{\tau_U - \tau(t)}{\tau_U - \tau_L}\alpha_1 + \frac{\tau(t) - \tau_L}{\tau_U - \tau_L}\alpha_2\Big)(A_i\hat{G}^T + \hat{G}A_i^T) + \hat{Q} + \hat{R}_1 + \hat{R}_2,$$

$$\hat{\pi}_{12}^{ij\tau(t)} = \Big(\frac{\tau_U - \tau(t)}{\tau_U - \tau_L}\beta_1 + \frac{\tau(t) - \tau_L}{\tau_U - \tau_L}\beta_2\Big)\hat{G}A_i^T + \Big(\frac{\tau_U - \tau(t)}{\tau_U - \tau_L}\alpha_1 + \frac{\tau(t) - \tau_L}{\tau_U - \tau_L}\alpha_2\Big)B_iL_j + \hat{M}_1 - \hat{N}_1,$$

$$\hat{\pi}_{13}^{ij\tau(t)} = (\tau_U - \tau(t))(\hat{X}_1 + \hat{X}_2^T) - \hat{M}_1, \quad \hat{\pi}_{14}^{ij\tau(t)} = (\tau_U - \tau(t))\hat{X}_3 + \hat{N}_1,$$

$$\hat{\pi}_{15}^{ij\tau(t)} = \hat{P} - \Big(\frac{\tau_U - \tau(t)}{\tau_U - \tau_L}\alpha_1 + \frac{\tau(t) - \tau_L}{\tau_U - \tau_L}\alpha_2\Big)\hat{G} + \Big(\frac{\tau_U - \tau(t)}{\tau_U - \tau_L}\gamma_1 + \frac{\tau(t) - \tau_L}{\tau_U - \tau_L}\gamma_2\Big)\hat{G}A_i^T + (\tau_U - \tau(t))(\hat{X}_1 + \hat{X}_1^T),$$

$$\hat{\pi}_{16}^{ij\tau(t)} = \Big(\frac{\tau_U - \tau(t)}{\tau_U - \tau_L}\lambda_1 + \frac{\tau(t) - \tau_L}{\tau_U - \tau_L}\lambda_2\Big)\hat{G}A_i^T - \Big(\frac{\tau_U - \tau(t)}{\tau_U - \tau_L}\alpha_1 + \frac{\tau(t) - \tau_L}{\tau_U - \tau_L}\alpha_2\Big)B_iL_j,$$

$$\hat{\pi}_{17}^{ij} = \hat{X}_1 + \hat{X}_2^T, \quad \hat{\pi}_{18}^{ij} = -\hat{X}_3,$$

$$\hat{\pi}_{22}^{ij\tau(t)} = \hat{M}_2 + \hat{M}_2^T - \hat{N}_2 - \hat{N}_2^T + 2\Big(\frac{\tau_U - \tau(t)}{\tau_U - \tau_L}\beta_1 + \frac{\tau(t) - \tau_L}{\tau_U - \tau_L}\beta_2\Big)B_iL_j + \epsilon\Phi,$$

$$\hat{\pi}_{23}^{ij} = -\hat{M}_2 + \hat{M}_3^T - \hat{N}_3^T, \quad \hat{\pi}_{24}^{ij} = \hat{N}_2 - \hat{N}_4^T + \hat{M}_4^T,$$

$$\hat{\pi}_{25}^{ij\tau(t)} = -\Big(\frac{\tau_U - \tau(t)}{\tau_U - \tau_L}\beta_1 + \frac{\tau(t) - \tau_L}{\tau_U - \tau_L}\beta_2\Big)\hat{G} + \Big(\frac{\tau_U - \tau(t)}{\tau_U - \tau_L}\gamma_1 + \frac{\tau(t) - \tau_L}{\tau_U - \tau_L}\gamma_2\Big)L_j^TB_i^T,$$

$$\hat{\pi}_{26}^{ij\tau(t)} = -\Big(\frac{\tau_U - \tau(t)}{\tau_U - \tau_L}\beta_1 + \frac{\tau(t) - \tau_L}{\tau_U - \tau_L}\beta_2\Big)B_iL_j + \Big(\frac{\tau_U - \tau(t)}{\tau_U - \tau_L}\lambda_1 + \frac{\tau(t) - \tau_L}{\tau_U - \tau_L}\lambda_2\Big)L_j^TB_i^T - \epsilon\hat{\Phi},$$

$$\hat{\pi}_{33}^{ij} = -\hat{R}_1 - \hat{M}_3 - \hat{M}_3^T, \quad \hat{\pi}_{34}^{ij} = -\hat{M}_4^T + \hat{N}_3, \quad \hat{\pi}_{37}^{ij\tau(t)} = -(\tau_U - \tau(t))(\hat{X}_2 + \hat{X}_2^T),$$

$$\hat{\pi}_{38}^{ij\tau(t)} = -(\tau_U - \tau(t))\hat{X}_4, \quad \hat{\pi}_{44}^{ij} = -\hat{R}_2 + \hat{N}_4 + \hat{N}_4^T,$$

$$\hat{\pi}_{47}^{ij\tau(t)} = (\tau_U - \tau(t))\hat{X}_4, \quad \hat{\pi}_{48}^{ij\tau(t)} = (\tau_U - \tau(t))\hat{X}_5, \quad \hat{\pi}_{55}^{ij\tau(t)} = -\Big(\frac{\tau_U - \tau(t)}{\tau_U - \tau_L}\gamma_1 + \frac{\tau(t) - \tau_L}{\tau_U - \tau_L}\gamma_2\Big)(\hat{G} + \hat{G}^T) + \tau^*\hat{S},$$

$$\hat{\pi}_{56}^{ij\tau(t)} = -\Big(\frac{\tau_U - \tau(t)}{\tau_U - \tau_L}\lambda_1 + \frac{\tau(t) - \tau_L}{\tau_U - \tau_L}\lambda_2\Big)\hat{G}^T - \Big(\frac{\tau_U - \tau(t)}{\tau_U - \tau_L}\gamma_1 + \frac{\tau(t) - \tau_L}{\tau_U - \tau_L}\gamma_2\Big)B_iL_j,$$

$$\hat{\pi}_{57}^{ij\tau(t)} = -(\tau_U - \tau(t))(\hat{X}_1^T + \hat{X}_2), \quad \hat{\pi}_{58}^{ij\tau(t)} = (\tau_U - \tau(t))\hat{X}_3,$$

$$\hat{\pi}_{66}^{ij\tau(t)} = -\Big(\frac{\tau_U - \tau(t)}{\tau_U - \tau_L}\lambda_1 + \frac{\tau(t) - \tau_L}{\tau_U - \tau_L}\lambda_2\Big)(\hat{G} + \hat{G}^T) + (\epsilon - 1)\hat{\Phi},$$

$$\hat{\pi}_{77}^{ij} = -(\hat{X}_2 + \hat{X}_2^T), \quad \hat{\pi}_{78}^{ij} = -\hat{X}_4,$$

$$\hat{\pi}_{88}^{ij} = -\hat{X}_5 \text{ and } \tau^* = \tau_U - \tau_L.$$